Politecnico di Torino
Master of Science in Materials Engineering for Industry 4.0

Master's Thesis

Lignin-Derived Free-Standing Carbon Mats for Glycerol Electrooxidation

Academic Year 2025/2026

Supervisors
Prof. Marco Sangermano
Prof. Maria Magdalena Titirici
Dr. Robert Hunter
Hanzhi Ye PhD Candidate

Candidate
Giovanni Smoqi

Master's Thesis carried out at
Imperial College London

March 2026

Table of Contents

1 Chapter 1 – Introduction

1.1 Aim of the Thesis

The global shift toward a more sustainable and circular economy cannot be achieved only by improving existing technologies but also requires a rethinking of the materials and processes that underpin modern industrial systems. In this context, carbon-based components play a central role, especially in electrochemical devices such as fuel cells, electrolyzers and electrochemical reactors [1], [2]. Despite this, most high-performance carbon materials currently used in these systems are derived from fossil resources and rely on energy-intensive manufacturing routes [3].
This thesis is positioned at the intersection of this contradiction, addressing the question of whether a low-value industrial by-product such as lignin can be transformed into a functional and sustainable carbon substrate capable of replacing conventional fossil-derived materials in electrochemical applications.
Lignin is produced in very large quantities as a by-product of the pulp and paper industry and emerging biorefineries, and it is still predominantly burned on-site for process heat, representing a low-value end use [4], [5]. This is in contrast with its intrinsic chemical structure: lignin is an aromatic, carbon-rich biopolymer that, in principle, represents an excellent precursor for carbon materials [2]. At the same time, state-of-the-art carbon substrates used in electrochemical systems, such as carbon papers, carbon cloths and porous carbons, are typically produced from petroleum-based polymers or pitch through multi-step processes involving oxidative stabilization, high-temperature carbonization and, in some cases, graphitization or activation [3], [6]. These routes are energetically demanding and environmentally intensive, which partially undermines the sustainability of electrochemical technologies that are otherwise considered "green".
The central ambition of this thesis is to investigate lignin as a viable precursor for advanced carbon mats specifically designed to act as electrode substrates. The goal is not limited to demonstrating that lignin can be converted into carbon, but rather to assess whether lignin-derived architectures can meet the set of requirements demanded by practical electrochemical devices. These include sufficient electrical conductivity, appropriate surface chemistry, interconnected porosity for mass transport, and structural integrity under handling and operation [2], [3], [7]. Several challenges are immediately apparent. Lignin is chemically and structurally heterogeneous, with properties that strongly depend on botanical origin and extraction method, which complicates its processing into uniform fibers or continuous networks [8]. In addition, carbonization of biopolymers often leads to brittle structures unless morphology and processing parameters are carefully controlled [3]. Moreover, an electrode substrate does not act as a passive support. Its pore structure, surface chemistry and electron transport pathways directly influence catalyst utilization, mass transport and long-term stability during electrochemical operation [1], [9]. For this reason, lignin must be approached not only as a "green" precursor, but as a materials design challenge. Its aromatic backbone and oxygen-rich functional groups can be exploited to engineer tailored carbon frameworks, provided that precursor formulation, fiber or mat formation and thermal treatment are properly controlled.
Within this framework, the work is organized around three main objectives:

1. **To show, from both a scientific and practical perspective, why lignin can be considered a sustainable alternative to fossil-based carbon substrates.** This includes discussing lignin's intrinsic aromaticity as a carbon precursor, its position within circular material flows, and its potential advantages in terms of biogenic origin, availability and tunable chemistry for electrochemical applications
2. **To develop and study processing routes that convert lignin into mechanically robust, conductive and hierarchically porous carbon mats.** Rather than optimizing individual steps in isolation, the thesis focuses on the interplay between lignin source, solution formulation, fiber or mat formation by electrospinning, and carbonization conditions, and how these parameters collectively determine morphology, porosity and electrical properties.

3. **To evaluate the performance of lignin-derived carbon mats as functional electrode substrates in realistic electrochemical environments.** The aim is to assess not only their electrochemical response, but also their ability to act as free-standing substrates capable of supporting catalyst layers and competing with commercial fossil-derived carbon papers under biomass electro-oxidation conditions.

Taken together, these objectives define the scope of the thesis: to demonstrate that lignin can move beyond its current role as a low-value industrial residue and be transformed into a tunable carbon substrate suitable for electrochemical devices, while remaining aligned with principles of sustainability and circular economy. Ultimately, this work aims to show that the carbon backbone of future electrochemical systems does not necessarily need to originate from finite fossil resources but can instead be built from the complex molecular architecture of renewable biomass.

1.2 Energy transition and the role of biomass electro-oxidation: the case of glycerol oxidation (GOR)

The development of lignin-derived carbon substrates is connected to the broader shift towards low-carbon energy technologies. In this context, electrochemical routes are increasingly explored to replace fossil-based processes, but their actual sustainability depends not only on device efficiency, but also on the choice of electrode materials and on the reactions occurring at their surfaces [1]. Conventional anodic reactions, such as the oxygen evolution reaction (OER), are often energy-intensive, kinetically sluggish, and produce oxygen as a low-value product, which limits the overall efficiency and economic attractiveness of electrochemical systems [10], [11].

The electro-oxidation of biomass-derived molecules offers an alternative anodic pathway, where renewable feedstocks can be converted while delivering useful currents and, at the same time, generating value-added products [11], [12], [13]. In this sense, biomass and organic electro-oxidation reactions have attracted increasing interest as a strategy to reduce cell voltages and improve the overall sustainability of electrochemical processes [10].

Section 1.2.1 outlines the role of electrochemical routes in the energy transition, Section 1.2.2 introduces biomass and organic electro-oxidation as alternative anodic processes, and Section 1.2.3 focuses on glycerol electro-oxidation as the specific case considered in this work.

1.2.1 Brief overview of energy transition and electrochemical routes

The world is moving toward a decarbonized energy system, as many countries commit to net-zero carbon emission targets and the progressive phase-out of fossil fuels in favour of renewable and sustainable energy sources [14], [15]. However, a major challenge associated with most renewable energy sources is their intermittent nature and limited dispatchability. Energy storage and energy conversion technologies are therefore essential to mitigate these limitations, by balancing temporal mismatches between energy generation and demand and by enabling the transformation of renewable electricity into storable and versatile energy carriers [15].

Addressing the intermittency of renewable energy sources requires a broader system-level strategy that includes grid expansion and interconnection, demand-side management and sector coupling. Within this framework, electrochemical technologies play a central role and a schematic of how they help achieve a cleaner future is shown in Figure 1. Fuel cells and electrolyzers are widely investigated for energy conversion, while batteries and supercapacitors are employed for electrical energy storage [1], [2]. These devices either use renewable electricity directly to drive chemical reactions or convert fuels and biomass into electricity at temperatures significantly lower than those required by conventional combustion processes.

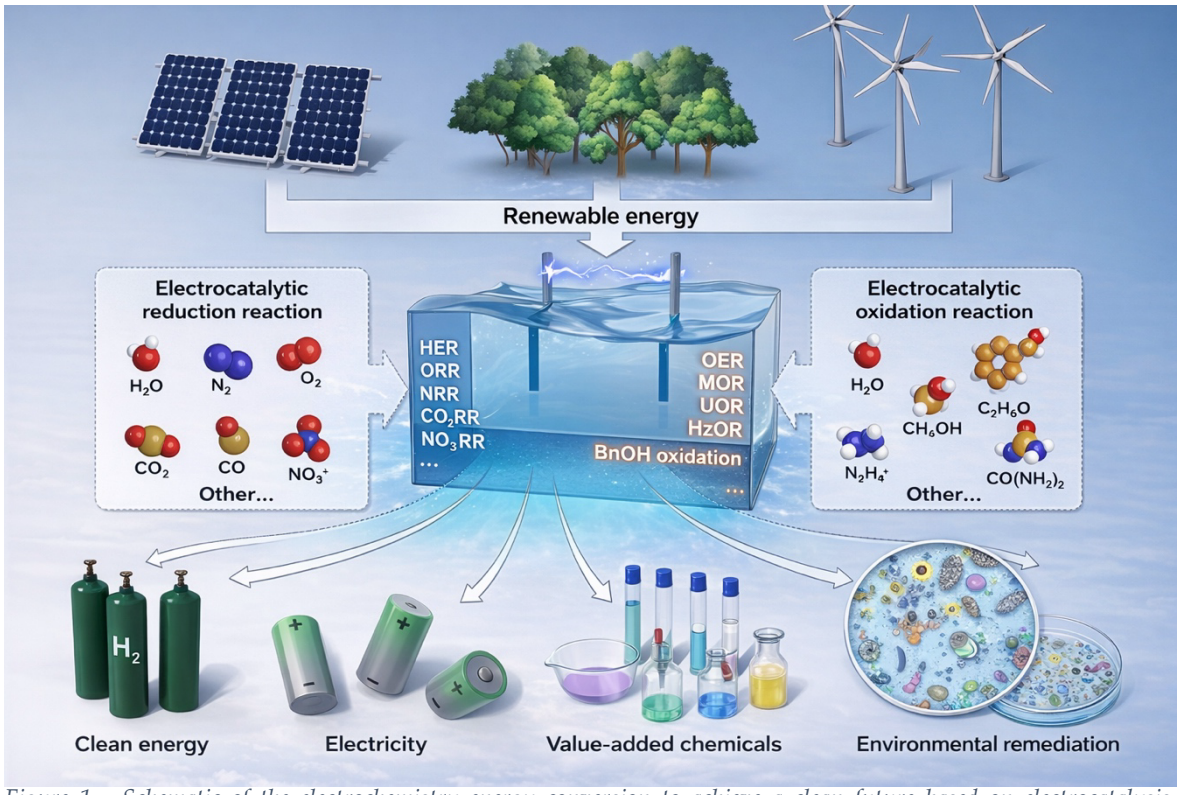

Figure 1 - Schematic of the electrochemistry energy conversion to achieve a clean future based on electrocatalysis. Reproduced from [16]

Despite their potential to enable a low-carbon energy system, most electrochemical devices still rely on high-performance materials derived from fossil feedstocks, such as carbon paper, carbon cloth and various types of porous carbons. A full energy transition therefore requires the replacement of these materials with renewable and biogenic alternatives. Recent literature has shown that lignin-derived carbons can effectively substitute fossil-based carbons in several electrochemical applications, including supercapacitor electrodes, battery anodes and catalyst supports [2], [7].
This line of reasoning can be extended beyond the choice of materials to the efficiency of anodic reactions themselves. In particular, replacing the oxygen evolution reaction (OER) with the electro-oxidation of biomass-derived organic molecules has emerged as an attractive strategy, as it can reduce the energy required to operate electrolytic systems while simultaneously enabling the production of higher-value chemicals [10], [11], [13]. This concept is further explored in the following sections.

1.2.2 Biomass electro-oxidation and organic oxidation reactions as alternative anodic processes

The OER is the standard anodic reaction in water electrolysis, but it suffers from several drawbacks: it is kinetically sluggish, it requires a high overpotential, and it generates oxygen, a product with limited economic value [17]. Alternative anodic reactions have therefore attracted increasing attention, as they can be easier to drive, operate at lower overpotentials, and lead to more valuable reaction products. In this context, organic molecules such as alcohols and polyols can effectively replace water at the anode, and many of these compounds are derived directly from biomass or from biomass processing streams. When such species are oxidized at the anode, the overall process is typically referred to as organic oxidation reactions or, more specifically, biomass electro-oxidation [10], [11], [12], [18].

The advantages of these reactions can be described along two main axes. From an energetic point of view, the onset potentials required for the oxidation of many organic substrates are significantly lower than those for OER, so the cell voltage can be reduced and the overall

energy consumption of the electrochemical process decreases. From the product perspective, the electro-oxidation of biomass-derived molecules often yields value-added chemicals such as acids, aldehydes or other functionalized intermediates. In this way, the anode is no longer a site that produces only low-value oxygen but becomes a platform for the co-production of higher-value chemicals, as shown in Figure 2 where the organic molecule in question is glycerol.

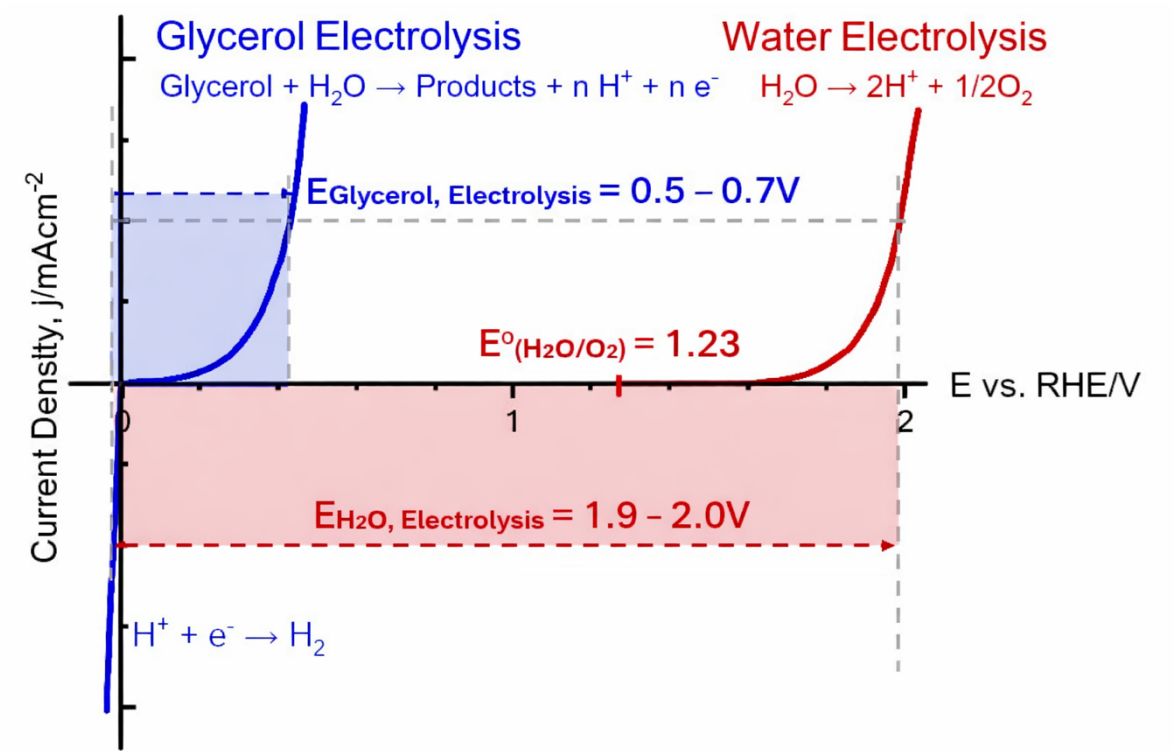

Figure 2 - Thermodynamics and kinetics for water electrolysis and glycerol electrolysis. The glycerol electrooxidation (GOR) delivers value added products, whereas the oxygen evolution reaction only produces oxygen. Furthermore, the theoretical thermodynamic oxidation potential is much lower for the GOR, making the cell's required energy decrease relatively to the OER. Adapted from [13]

The practical implementation of biomass electro-oxidation requires appropriately formulated electrolytes and carefully selected materials for both catalysts and electrode substrates. In particular, the anodic substrate must provide high electrical conductivity, suitable porosity and mass-transport properties, and long-term stability under operating conditions. At present, these requirements are usually met by carbon materials produced from fossil feedstocks, although there is a clear shift toward biogenic and waste-derived alternatives. Among the various biomass-derived substrates investigated for such alternative anodic processes, glycerol has emerged as a particularly attractive case, because it combines a favourable effect on cell efficiency with the possibility of generating a spectrum of higher-value oxidation products.

1.2.3 Glycerol electro-oxidation (GOR) as a representative case

Glycerol is one of the most relevant biomass-derived polyols, as it is produced in large amounts as a by-product of the biodiesel and oleochemical industries. It is cheap, non-toxic, water-soluble and already available in large existing streams, which makes it a natural candidate for electro-oxidation studies. From an electrochemical point of view, glycerol is attractive because its multiple hydroxyl groups and high oxygen content allow for rich redox chemistry, and its oxidation can be combined with hydrogen evolution or other cathodic reactions in low-voltage electrolysis concepts [10], [11], [18].

The glycerol electro-oxidation reaction (GOR) has therefore been widely investigated on different noble-metal catalysts, mainly Pt- and Pd-based systems supported on carbon. Most work is carried out in alkaline media, using electrolytes such as KOH or NaOH containing glycerol in various concentrations, and applying potential windows where glycerol oxidation occurs at substantially lower potentials than OER. Under these conditions, GOR can lower the overall cell voltage compared to conventional water splitting and, at the same time, generate a broad distribution of partial oxidation products. Depending on catalyst composition, potential and reaction environment, products such as glycerate, glycolate, lactate and other C_1–C_3 species are typically reported [10], [11], [19]. A simplified overview of glycerol electro-oxidation pathways is shown in Figure 3.

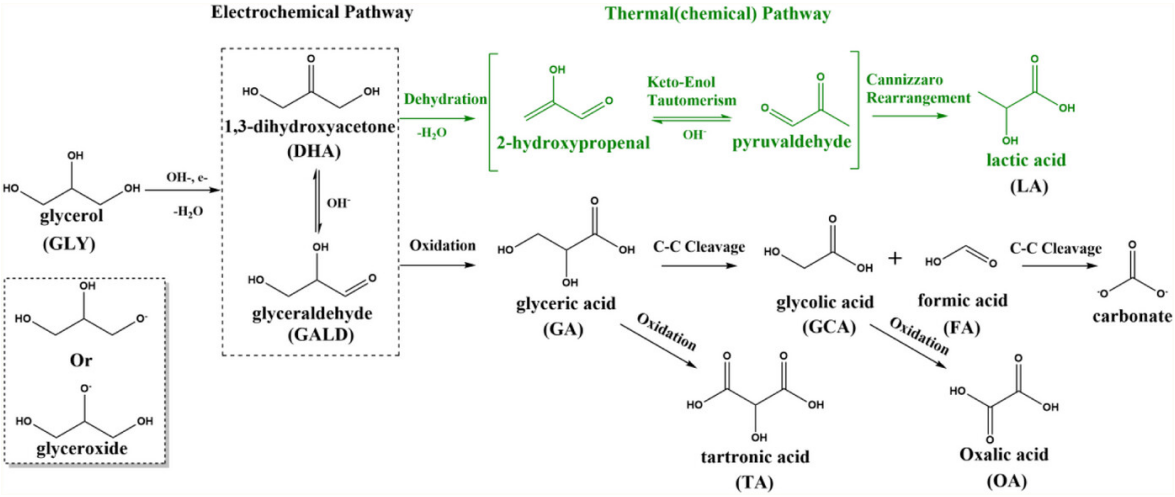

Figure 3 - Reaction pathway for glycerol electro-oxidation, consisting of electrochemical pathways (black) and thermal-chemical pathway (green). Reproduced from [20]

However, GOR is a complex reaction system, as the selectivity is highly sensitive to the catalyst surface, and deactivation phenomena such as poisoning by strongly adsorbed intermediates are frequently observed. As a result, the performance of a given GOR system cannot be described only in terms of the active metal phase. The properties of the underlying electrode substrate, including its electrical conductivity, porosity, wettability and surface chemistry, play a central role in controlling mass transport, local environment and effective utilization of the catalyst layer.

For these reasons, glycerol electro-oxidation is often used as a benchmark reaction to test new catalyst formulations and electrode architectures. In this context, GOR represents a useful probe reaction to evaluate electrode substrates. The reaction involves complex mass transport phenomena, catalyst utilization effects, and surface poisoning processes, all of which are strongly influenced by the underlying carbon architecture. As a result, GOR provides a relevant electrochemical environment to assess whether lignin-derived mats can operate as functional electrode substrates [13]. In this thesis, GOR is not the primary topic in itself, but rather a representative anodic reaction chosen to probe the suitability of lignin-derived electrospun carbon mats as electrode substrates and to compare their behaviour with that of conventional fossil-derived carbon supports.

1.3 Carbon substrates for electrochemical devices: from fossil-derived supports to bio-based alternatives

The role of carbon substrates in electrochemical technologies is not passive, as they enable electron pathways, mass transport, mechanical integrity, and wettability. They play a key role in fuel cells, electrolyzers, CO_2 reduction cells, and GOR electrodes.
Most carbon substrates are fossil-fuel-derived, as they are produced from polyacrylonitrile (PAN), pitch, or other petrochemical derivatives, and their manufacturing typically involves energy-intensive processes. Thus, even if the targeted reaction is green, the

substrate itself is not. The ultimate challenge is to understand whether fossil-based supports can be completely replaced by greener options.
The following sections describe conventional carbon substrates (1.3.1), discuss the essential requirements a substrate must meet (1.3.2), and highlight their limitations in terms of sustainability and circular economy (1.3.3).

1.3.1 Conventional carbon papers and gas diffusion layers (GDLs)

In many electrochemical devices, especially fuel cells and electrolyzers, electrodes are made of gas diffusion layers (GDLs) based on carbon paper or carbon cloth. The GDL provides various properties, such as porosity and microporosity balanced with adequate wettability, and coordinates the transport of fluids in its porous network. Similar substrates are used as the foundation of electrocatalytic electrodes in reaction like the oxygen evolution reaction or glycerol oxidation reaction [9], [10].
Commercial GDLs are usually composed of a macroporous layer made of carbon cloth or carbon paper, derived from PAN or pitch, and a microporous layer enriched with carbon black and hydrophobic agents to grant the right balance of wettability (Figure 4). The former layer's functions are mechanical support, in-plane conductivity and a pore structure that is engineered to both permit gas permeation and also maintain the catalyst attached and stable.

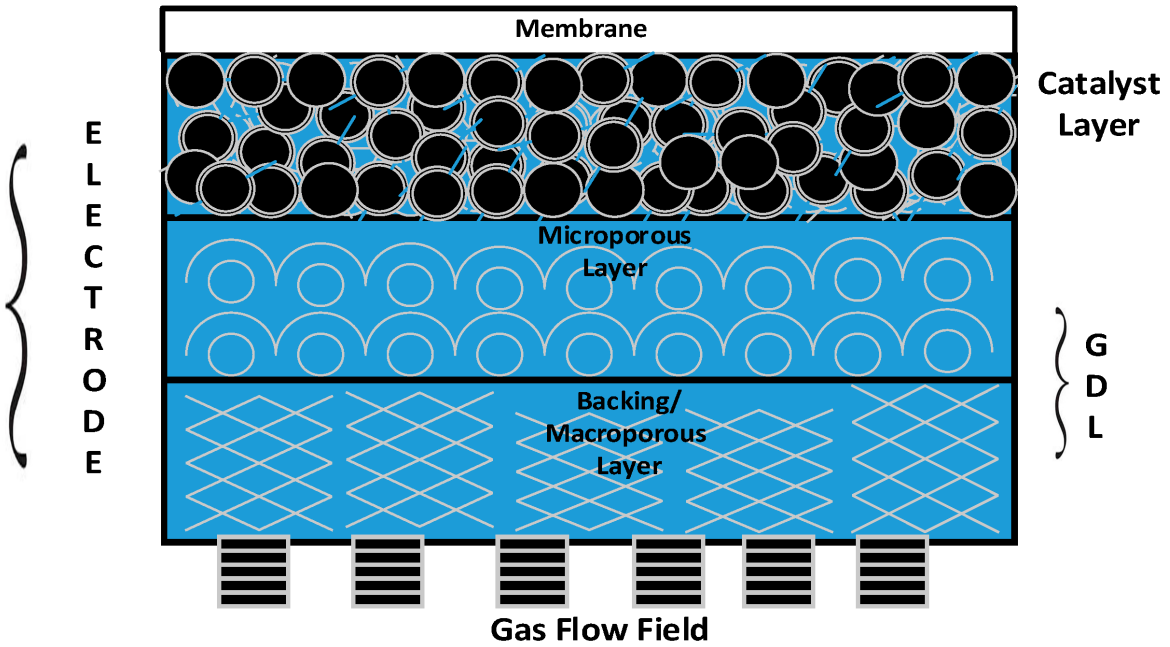

Figure 4 - A 2D view of a gas diffusion electrode (GDE) indicating the catalyst layer and gas diffusion layer (GDL; comprising a backing layer and mesoporous layer, MPL). Reproduced from [21]

To tailor wettability and liquid transport inside the carbon network, various surface treatments are applied, for example fluorinated polymers coatings, such as PTFE or PVDF [9]. In PEM fuel cells, GDLs are vastly used and their performance has been heavily documented in literature; the same substrated are employed in biomass fuel cells and electrocatalytic polyols oxidation studies, as they're usually sprayed with noble metals, like Pt or Pd, and then tested for their performance [11], [19]. Furthermore, the anodic acitivity is not only linked to the catalyst sprayed on it but also largely to its intrinsic structure, porous network and surface characteristics. Understanding how performance is sensibly defined by all this aspects, allows actual assessment of wether alternatives can take their place or not.

1.3.2 Structural and functional requirements for electrode substrates

Electrode substrates need to meet specific requirements to be effective. First, high in-plane electrical conductivity is required to minimize ohmic losses, which can lead to different operative potentials along the electrode, resulting not only in underutilisation of the

catalyst, but also in altered selectivity and reduced stability. Second, an adequate porosity and pore size distribution are key to ensuring proper mass transport of reactants, products and electrolyte. The pores must have appropriate sizes and related tortuosity, so that reactants and products can effectively reach and leave the catalyst layer without creating dead zones or transport limitations. Importantly, in electrode substrate design the objective is not necessarily to maximize surface area, but rather to achieve a balanced pore architecture that ensures efficient mass transport while maintaining electrical continuity and structural stability. Furthermore, a controlled wettability and a suitable hydrophilic/hydrophobic balance are fundamental to avoid both flooding and dry conditions. Mechanical robustness is also needed, as the substrate must be free-standing and able to support the catalyst layer deposited on top of it [5], [6], [22]. Finally, the surface chemistry must be carefully controlled in order to enable catalyst anchoring, resist corrosion and avoid undesired adsorption of reaction products during operation. These requirements are widely discussed for conventional GDLs and carbon substrates in fuel cells and electrochemical energy systems and they are summarized in Figure 5 [3], [6], [7], [23].

Figure 5 - Requirements for electrode substrates. Illustration by author.

1.3.3 Limitations of fossil-derived carbon substrates (sustainability, circularity, cost)

The main advantages of substrates derived from fossil-based precursors are accompanied by several limitations due to their intrinsic nature. Carbon papers and carbon cloths are mainly based on polyacrylonitrile (PAN), pitch and other petrochemical polymers [22], [23] The processes used to produce them are highly energy-demanding and involve slow oxidative stabilisation, high-temperature carbonisation and, in some cases, an additional final graphitisation or activation step [6]. Even if the reaction they sustain is effectively "green", the support itself remains fossil-derived, and this creates a strong inconsistency with the concept of circular economy and with the idea of having bio-based feedstocks.
This is where a material such as lignin comes into play: a biopolymer that is produced as a waste stream in millions of tonnes per year, usually burned for low-value heat, but that can in fact be transformed into a functional material with interesting properties that can be exploited in electrochemical applications [5], [24]. Despite this potential, lignin-derived carbons have mainly been studied as electrodes in supercapacitors, as anodes for batteries and as rather generic catalyst supports, but not directly as free-standing substrates for reactions such as glycerol oxidation [2], [5]. It is precisely this gap that the present thesis aims to address.

1.4 Lignin: structure, availability and valorization routes

Lignin is one of the major components of plant cell walls and is an aromatic, highly cross-linked polymer derived from phenylpropanoid monomers [5], [6], [8]. Despite the umbrella term "lignin", multiple lignin types exist, depending on biosynthetic pathways, botanical source and extraction method, and it has been shown that certain sources contain monomeric units that are not present in all lignins. There is an active research effort aimed at defining the extraordinary diversity of lignin structures and at exploring how they can be engineered [8].
In the context of this thesis, a detailed analysis of lignin chemistry is not strictly necessary, but it is important to recognise that its aromatic and heterogeneous nature has direct consequences for its behaviour as a precursor of carbon mats and opens up many possibilities for engineering a complex system with numerous variables [22]. The following sections summarise its main structural features (1.4.1), global availability (1.4.2) and the most relevant valorisation routes, with a focus on carbon materials (1.4.3).

1.4.1 Chemical structure and types of lignin

Lignin is a three-dimensional, amorphous polyphenolic polymer that sits in the plant cell wall together with cellulose and hemicellulose. From a chemical point of view, it is mainly built from three aromatic phenylpropane units: p-hydroxyphenyl (H), guaiacyl (G) and syringyl (S), which come from the corresponding monolignols p-coumaryl, coniferyl and sinapyl alcohol [5], [8]. These units are linked to each other through a combination of C–O and C–C bonds, where the β–O–4 aryl ether linkage is usually the most abundant, together with other motifs such as β–5, 5–5 and β–β [8], [22]. The result is a highly cross-linked and irregular network, with different hydroxyl, methoxy and carbonyl groups distributed along the structure (Figure 6).

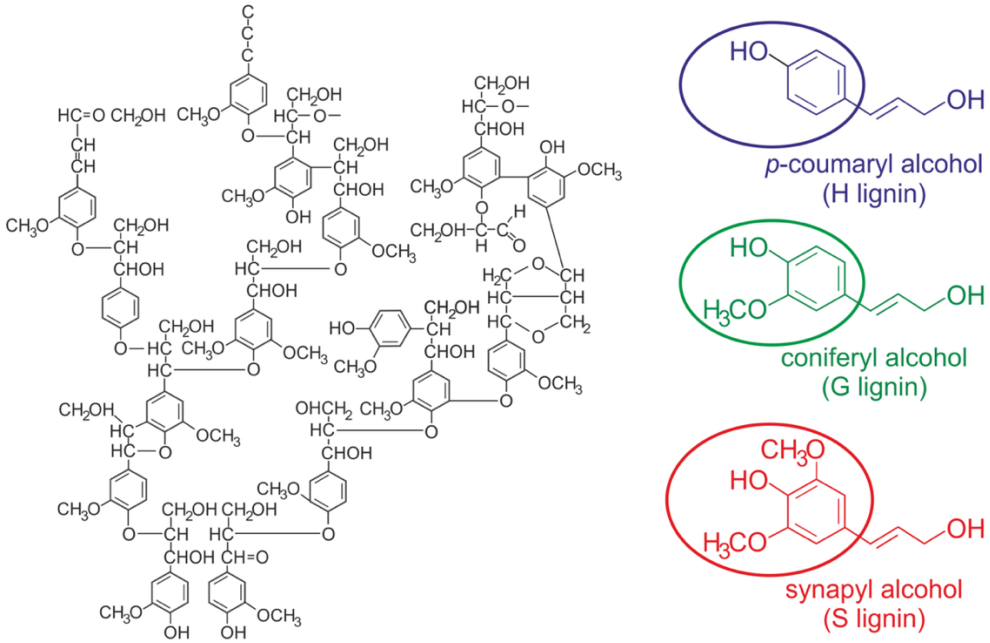

Figure 6 - Basic structure of lignin in lignocellulosic biomass (left). Different phenylpropane units of lignin (right): p-coumaryl alcohol (p-hydroxyphenyl unit, blue circle), coniferyl alcohol (guaiacyl unit, green circle) and sinapyl alcohol (syringyl unit, red unit). Reproduced from [25]

The percentage of lignin and relative amount of H, G and S units is not fixed and depends on the plant source (Table 1): softwoods are typically rich in guaiacyl units, hardwoods contain mainly guaiacyl and syringyl units, while grasses and other monocots generally show all three, and can also carry additional phenolic moieties such as p-coumarates and ferulates [4], [8].

Table 1 - Lignin content and monomer composition in different biomass sources. Reproduced from [4]

Biomass	% **Lignin**	**Monomer (H, G, S)**
Jute stem	12–26	G & S
Hazelnut (HL) and walnut (WL) shells (agro-food lignin)	85–95	H, G & S
Picea abies wood	25–29	H, G & S
Pinus pinaster wood	23–30	H, G & S
Pinus pinaster bark	33	H, G & S
Phloem	38	H, G & S
Sapwood	32	H, G & S
Sugarcane bagasse	21	H, G & S
Wheat straw	22	G & S
Bamboo	25–27	H, G & S

On top of this natural variability, industrial extraction changes the lignin even further. Kraft, soda, organosolv and lignosulfonate lignins differ in terms of degree of condensation, sulphur content and type of functional groups, and these differences affect properties such as solubility, thermal behaviour and the carbon yield after pyrolysis [6], [22]. In this work an organosolv lignin is used as precursor, since it is generally considered cleaner, with a relatively high aromatic purity and lower inorganic and sulphur content. This makes it a suitable starting point to prepare carbon mats and to study how lignin structure influences the properties of the resulting lignin-derived carbon materials [2], [5].

1.4.2 Global production and current uses

Lignin is produced in very large amounts every year as a by-product of different industrial processes. The main industrial sources are the pulp and paper sector (for example Kraft and sulphite pulping) and, more recently, emerging biorefineries that process lignocellulosic biomass for second-generation biofuels and related products [1], [26]. On the technical side, i.e. for lignin that is actually isolated from process streams, the global production has been estimated at about 1.65 million tonnes per year in 2018, with lignosulfonates accounting for roughly 80% of this amount (around 1.3 million tonnes per year) and kraft lignin contributing approximately 0.27 million tonnes per year [4]. These figures are small compared to the total lignin present in lignocellulosic biomass worldwide, but they still represent a substantial and largely under-exploited resource.
In practice, the current use of industrial lignin is still dominated by low-value applications, at the bottom of the pyramid in Figure 7.

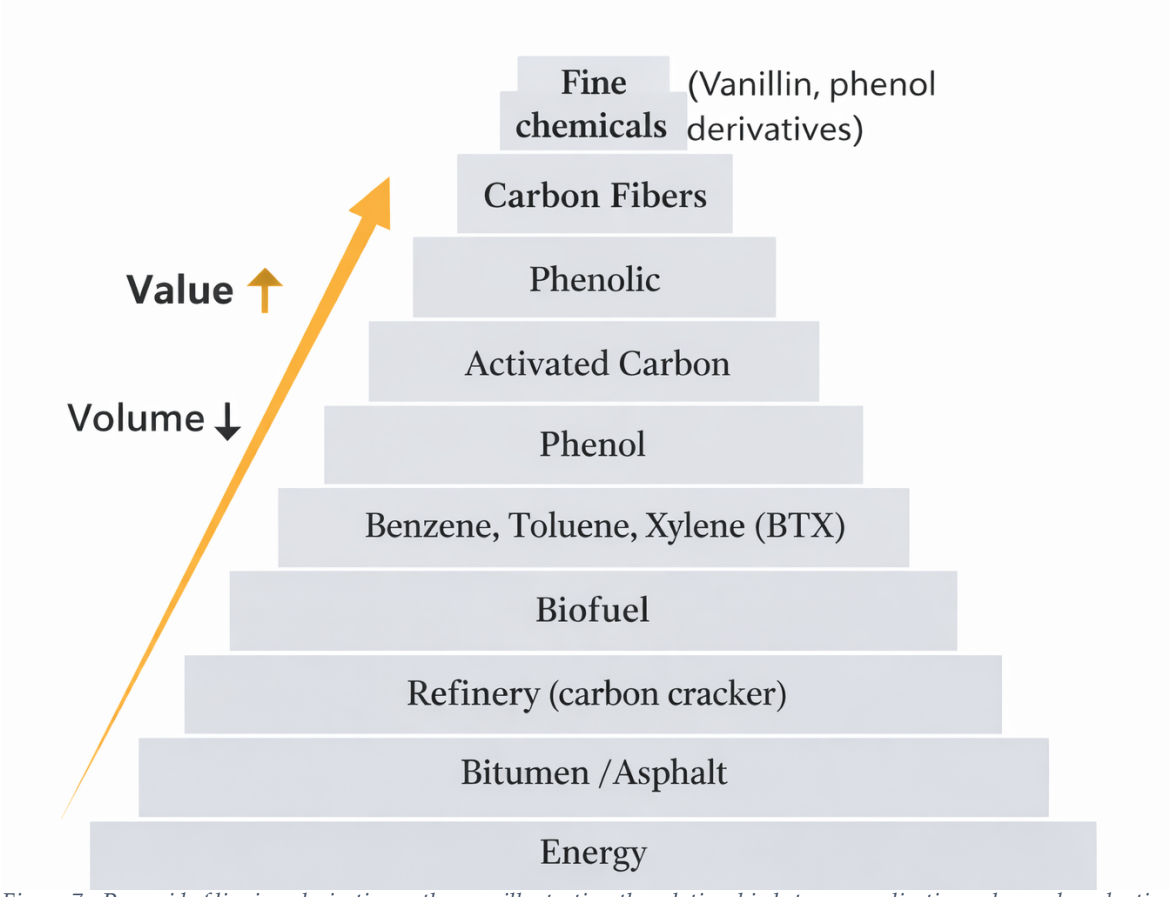

Figure 7 - Pyramid of lignin valorisation pathways, illustrating the relationship between application value and production volume. Lower levels correspond to high-volume, low-value uses (e.g., energy), while higher levels represent low-volume, high-value products such as fine chemicals. Adapted from [27]

In pulp and paper mills, most of the lignin contained in black liquor is simply burned on-site in recovery boilers to produce steam and process heat, with limited economic return [4], [5]. Energy recovery overall takes 95% of total produced lignin. Lignosulfonates have a more established market, mainly as dispersants, binders and additives in cement, concrete, and other formulations, but even in this case their use remains focused on bulk, low-margin products [2], [4]. Only a minor fraction of kraft lignin and other technical lignins is upgraded into higher-value products such as phenolic resins, polymer blends or advanced materials [28].
Using lignin merely as a fuel is acceptable from the point of view of local energy self-sufficiency in industrial plants, but it does not exploit the potential of its complex aromatic structure and does not maximise the value of its biogenic carbon content. In the context of the energy transition and circular economy, there is therefore increasing interest in lignin valorisation, including its conversion into functional carbon materials and polymers that can provide higher added value and help decouple advanced materials from fossil resources [1], [2], [29], [30].

1.4.3 Lignin valorization into carbon materials

Lignin valorization pathways have evolved significantly from simple combustion for heat recovery to sophisticated conversion into advanced carbon materials. While approximately 70–80% of technical lignin is still burned on-site in pulp mills for process energy, representing a low-value end-use, only 1–2% is currently upgraded into high-value carbon-based materials. This shift is driven by lignin's intrinsic aromatic structure—composed primarily of phenylpropane units—that provides a promising precursor for graphitizable carbons, unlike cellulosic materials which yield lower carbon contents. Global technical lignin production exceeds 50 million tonnes annually, yet only 1.5 million tonnes are isolated, presenting a vast untapped resource for sustainable carbon production [4], [5].

Pyrolytic routes represent the most established thermal valorization pathway, typically involving slow pyrolysis at 400–900 °C under inert atmosphere to produce biochar with carbon yields of 35–45 wt%. Subsequent chemical activation using KOH, H_3PO_4, or physical activation with CO_2 or steam at 700–1000 °C generates hierarchical porous carbons with specific surface areas ranging from 1000 to 3000 $m^2 g^{-1}$. These activated carbons excel in supercapacitor electrodes, achieving specific capacitances of 200–400 F g^{-1} and energy densities up to 15–20 Wh kg^{-1}, benefiting from both electric double-layer capacitance and pseudocapacitive contributions from residual oxygen/nitrogen heteroatoms. Hydrothermal carbonization (HTC) offers a milder aqueous route at 180–250 °C and autogenous pressure, producing uniform carbon microspheres without organic solvents, though with lower graphitization degrees [26].

Electrospinning emerges as the most relevant pathway for this thesis, enabling the production of continuous carbon nanofiber (CNF) mats with controlled morphology and hierarchical porosity. The process involves dissolving organosolv lignin (20–40 wt%) with carrier polymers such as polyethylene oxide (PEO, 5–20 wt%) in DMF/water or DMSO, followed by electrospinning at 15–25 kV, flow rates of 0.5–1.0 mL h^{-1}, and collector distances of 15–20 cm, yielding nanofibers with diameters of 200–800 nm. Oxidative stabilization at 200–300 °C in air induces crosslinking via dehydration and ether formation, preventing melting during subsequent carbonization at 800–1200 °C under nitrogen, which produces free-standing CNF mats with I_D/I_G ratios of 1.0–1.3 (Raman spectroscopy) indicative of turbostratic carbon structures [5], [26].

Properties of electrospun lignin-derived CNF mats typically include electrical conductivities of 10–100 S cm^{-1}, total porosities of 70–90%, and moderate surface areas (300–1000 $m^2 g^{-1}$), making them suitable for energy storage and catalyst supports. Mechanical reinforcement strategies, such as incorporation of 0.5–2 wt% multi-walled carbon nanotubes (MWCNTs), can increase tensile strength by 200–300% while enhancing both electrical and thermal conductivity. These mats have demonstrated excellent performance as supercapacitor electrodes (capacity retention >90% after 10,000 cycles) and Li-ion battery anodes (specific capacities 400 mAh g^{-1} at 1C), positioning them as viable alternatives to polyacrylonitrile (PAN)-derived carbon fibers [11], [29].

Emerging pathways include melt-spinning of low-melting-point alkali lignins, eliminating organic solvents for improved scalability, and catalytic chemical vapor deposition using lignin-derived tars to produce graphene-like structures. Heteroatom doping (N, P, S) during carbonization enhances electrocatalytic activity for oxygen reduction/evolution reactions, while template-directed synthesis yields ordered mesoporous carbons. These advanced routes expand lignin's application scope beyond traditional activated carbons [7].

Despite these advances, key limitations persist: carbonization yields remain low (20–40 wt% vs. 50% for PAN), electrospun mats exhibit brittleness requiring reinforcement, and precursor heterogeneity affects reproducibility. Critically, few studies have evaluated lignin-derived CNF mats as free-standing gas diffusion layer (GDL)-like substrates for electrocatalytic applications such as glycerol oxidation reaction (GOR), where balanced porosity-transport properties and mechanical integrity under operational stress are paramount. These gaps motivate the present work's focus on reinforced lignin mats benchmarked against commercial fossil-derived carbon substrates (Chapter 3) [8].

1.5 Lignin-derived carbon materials for electrochemical applications

Lignin-derived carbons have been explored in electrochemical technologies in a wide variety of architectures. Accordingly, the literature reports multiple forms, including activated carbons, aerogels, carbon fibers or carbon nanofibers (CNFs), and heteroatom-doped carbons [2], [7], [29]. This broad applicability is enabled by the intrinsic tunability of lignin-based materials, whose porosity, surface chemistry, and electrical conductivity can be tailored through appropriate processing strategies [5], [8], [22].

Based on this background, the present section is organized into three categories: lignin-derived porous carbons for energy storage applications, such as supercapacitors and batteries (Section 1.5.1); lignin-derived carbons employed as electrocatalyst supports or as

intrinsically electrochemically active materials (Section 1.5.2); and a critical positioning of lignin-derived carbons with respect to fossil-based benchmark substrates (Section 1.5.3).
Despite the extensive literature on lignin-derived carbons, most studies focus on powder-based or activated structures primarily optimized for high surface area, rather than on free-standing architectures engineered to function as electrode substrates [2], [7], [30]. In this context, the term *free-standing* refers to carbon architectures that are mechanically self-supported and do not require external current collectors or polymeric binders [3]. Although examples of self-supported lignin-derived carbons can be found in the literature, these systems are predominantly developed for supercapacitors, batteries, or as generic self-supported electrodes, and are not specifically designed to operate as electrode substrates comparable to commercial carbon papers [2], [3], [29].
When a carbon material is required to act as an electrode substrate, additional functional requirements arise. Beyond providing electrical conductivity, the substrate must enable efficient mass transport, ensure long-term mechanical and electrochemical stability, support catalyst deposition and adhesion, and ultimately allow for a meaningful comparison with commercial benchmark materials [6], [9], [22].
Since energy storage applications represent the most extensively investigated field for lignin-derived carbons, the discussion begins with these systems. This approach provides a well-established framework to elucidate key structure–property relationships, particularly concerning porosity, surface chemistry, and their influence on electrochemical performance.

1.5.1 Lignin-derived porous carbons for supercapacitors and batteries

Supercapacitors and batteries have represented the first and main testing ground for lignin-derived carbons. The primary reason is that these applications strongly reward high specific surface area, well-developed porosity, and tailored surface chemistry, all of which can be effectively achieved starting from lignin-based precursors [2], [7], [22], [30].
Within this context, several classes of lignin-derived carbons have been reported in the literature. These include activated carbons obtained through chemical or physical activation using potassium hydroxide, phosphoric acid, carbon dioxide, or steam; porous carbons and carbon aerogels; heteroatom-doped carbons containing nitrogen, phosphorus, sulfur, or oxygen; and, less frequently, lignin-derived carbon nanofibers (CNFs) produced via electrospinning or related techniques [22], [30].
The electrochemical performance of these materials in energy storage applications is highly promising. Reported specific surface areas commonly range from approximately 1000 up to more than 3000 $m^2 g^{-1}$, while specific capacitances are typically in the range of 200–400 F g^{-1}. In addition, excellent cycling stability is often achieved, with capacitance retention exceeding 90% after 5000–10,000 charge–discharge cycles. In battery-related studies, lignin-derived carbons also exhibit competitive specific capacities, in some cases approaching those of commercial activated carbons [2], [7], [30].
Despite these encouraging results, the corresponding carbon architectures are primarily optimized for charge storage rather than for continuous mass transport or for supporting catalyst layers. Therefore, they are frequently employed as powders, pressed electrodes, or binder-based systems, where the carbon material does not function as a structural electrode substrate [2], [7]. This makes their direct translation to substrate-based electrode configurations non-trivial, particularly for electrocatalytic applications where transport, mechanical integrity, and catalyst anchoring play a central role.
Building on the insights gained from energy storage studies, lignin-derived carbons have therefore also been explored as electrocatalyst supports and, in some cases, as intrinsically electrochemically active materials in a broader range of electrochemical and electrocatalytic reactions, as discussed in the following section.

1.5.2 Lignin-derived carbons as electrocatalyst supports

In electrocatalysis, the carbon support does not play a passive role and cannot be considered only as an electrical conductor, since it indirectly participates in the overall reaction. The carbon support strongly influences the dispersion of metal nanoparticles, their average size, and their stability against degradation processes such as sintering or dissolution. In

addition, the surface chemistry of carbon is crucial for metal–support interactions and can affect the adsorption of reaction intermediates or by-products. The structure of the carbon substrate may also present defects, exposed edge sites, or oxygen-containing functional groups. These features can improve catalyst anchoring and may influence the apparent selectivity of the catalyzed reaction. As a result, the carbon support indirectly modulates the catalytic system, and the metal–support interaction plays a key role in determining both catalytic performance and long-term stability (Figure 8) [1], [2], [7].

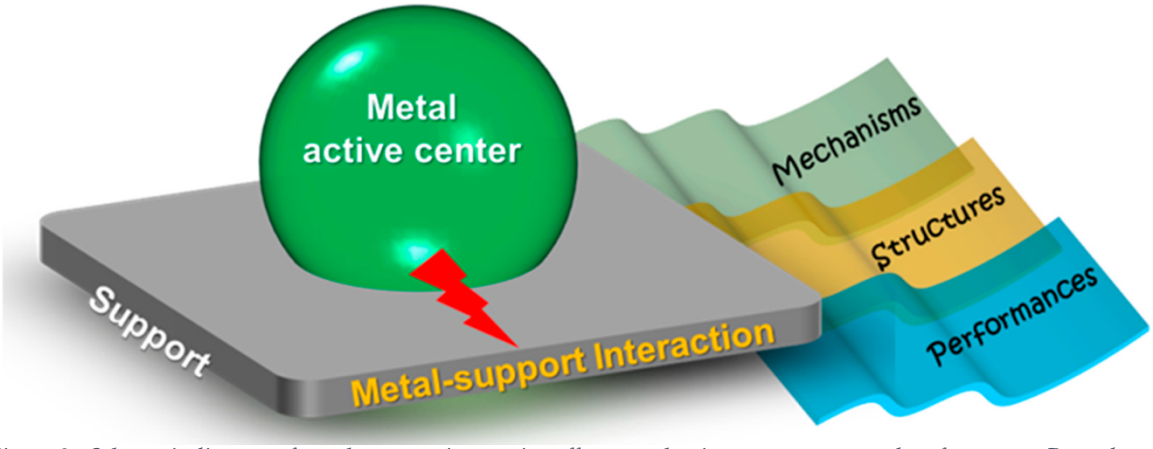

Figure 8 - Schematic diagram of metal–support interaction effects: mechanisms, structures, and performances. Reproduced from [17].

Numerous examples of this behavior can be found in the literature. Lignin-derived carbons have been employed as supports for platinum- or palladium-based catalysts in the oxidation of alcohols or polyols, as well as for nickel-, cobalt-, or iron-based catalysts in reactions such as the oxygen reduction reaction (ORR), oxygen evolution reaction (OER), and hydrogen evolution reaction (HER) [1], [7]. In many cases, a good metal dispersion is achieved, together with catalytic activities comparable to those obtained using conventional carbon black or Vulcan supports. Improved stability is often reported and is commonly attributed to favorable metal–support interactions. These interactions are promoted by surfaces rich in oxygen functional groups, defects, or heteroatoms, which facilitate nanoparticle nucleation, anchoring, and reduce catalyst detachment during operation [7], [17], [22].

Beyond their role as catalyst supports, lignin-derived carbons can also act as electrochemically active materials. In these cases, they exhibit intrinsic electrocatalytic activity, particularly when doped with heteroatoms such as nitrogen, phosphorus, or sulfur, or when characterized by a high density of defects and exposed edge sites. Typical reactions reported for such materials include metal-free ORR, assisted ORR, and surface redox processes associated with pseudocapacitive behavior [7], [17], [31].

Despite these promising results, several common limitations can be identified in the literature. From a structural point of view, most studies rely on carbon powders, activated carbons, or non-self-supporting materials. Electrodes are typically prepared as binder-based systems using Nafion or PVDF, or by drop-casting or spray-coating catalyst inks onto external supports. In these configurations, the lignin-derived carbon does not define the electrode substrate itself, but rather constitutes a component of a composite catalyst layer [2], [7]. From an experimental perspective, many investigations are conducted using idealized configurations such as rotating disk electrodes or H-cell setups, where it is difficult to clearly separate the role of the carbon architecture from that of the active catalyst [2], [12].

As a consequence, the carbon material is rarely evaluated as an electrode substrate, but instead as part of a catalyst layer. Key aspects such as mass transport through the carbon structure and mechanical integrity of the electrode are therefore seldom addressed. In particular, systematic studies on free-standing lignin-derived carbon mats functioning as electrode substrates are still limited, as well as direct comparisons with commercial carbon papers and applications in liquid-phase electrocatalysis, such as the glycerol oxidation reaction [12], [29], [32]. Overall, only limited attention has been devoted to these aspects.

1.5.3 Positioning lignin-derived carbons versus fossil-based benchmarks

To understand whether lignin-derived carbons can realistically replace fossil-based carbons, a complete comparison map is needed. This comparison should not be based only on electrochemical performance, but also on reproducibility, processability, and sustainability (Figure 9).

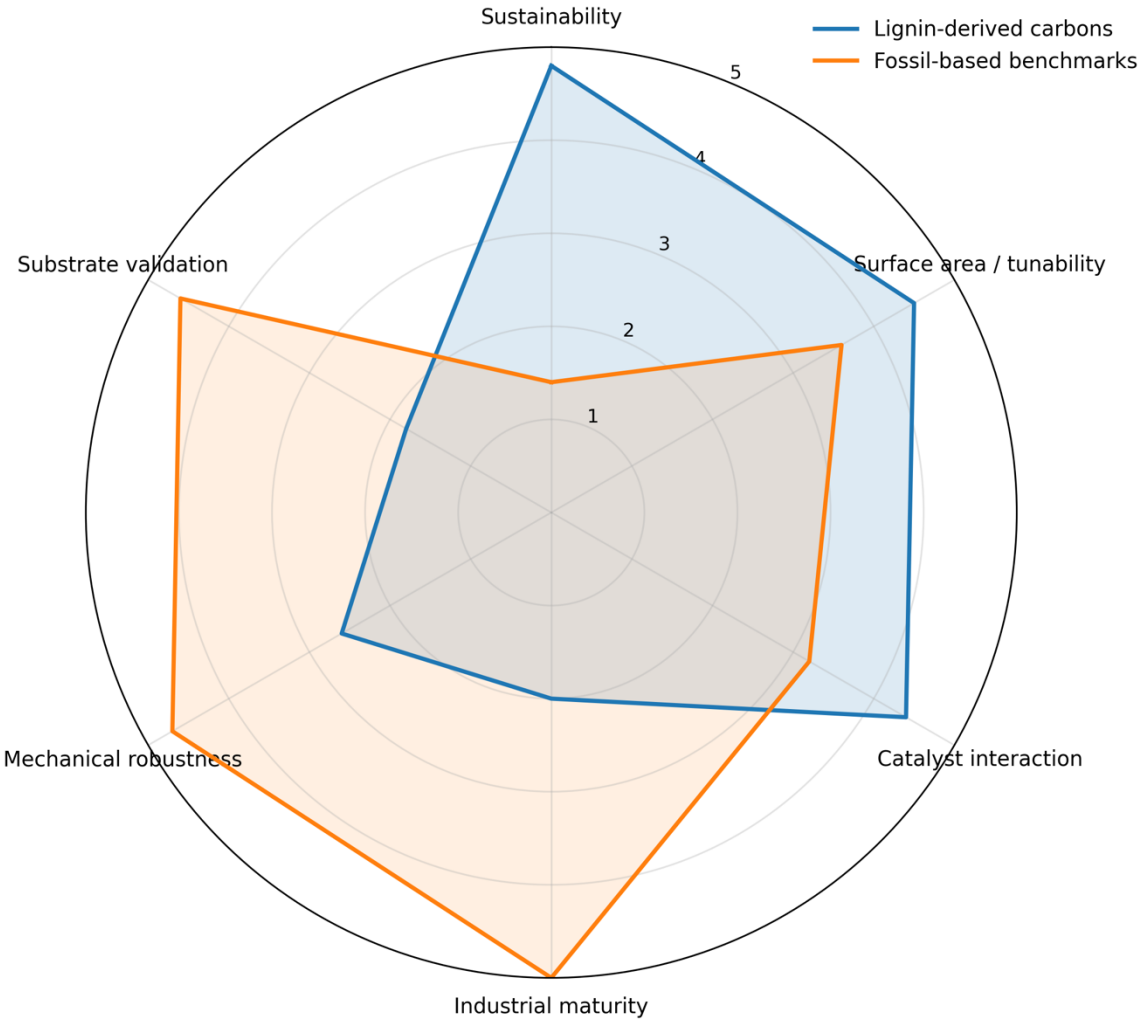

Figure 9 - Qualitative radar comparison between lignin-derived carbons and fossil-based benchmark substrates based on literature trends. Scores are normalized from 1 (low) to 5 (high) and are intended as a conceptual comparison rather than absolute measured values. Illustration by the author based on literature discussion in this section.

The most common fossil-based benchmarks include carbon blacks (e.g., Vulcan XC-72), commercial activated carbons, and carbon papers or cloths, often derived from PAN or pitch. These references are widely used because they offer high conductivity, good electrochemical stability, reproducibility, and established industrial processing routes, and they are also valued for their mechanical robustness in structural fiber-based forms. In particular, for PAN-based carbon fibres, the stabilization step is considered unavoidable and has been reported to account for about 48% of the total energy demand in PAN-CF production [33].

The literature shows that lignin-derived carbons can be highly competitive in several aspects: they can reach high surface areas, show rich surface chemistry, and provide favorable interactions with catalysts. In many applications, especially supercapacitors and batteries, performances are often comparable to commercial references, suggesting that lignin is not an intrinsic limitation but rather a highly tunable precursor. For instance, lignin-derived porous carbons can reach very high specific surface area (SSA) values, and it has been pointed out that specific capacitance does not necessarily continue increasing when SSA exceeds 2000 $m^2 g^{-1}$, even if SSA can approach 3000 $m^2 g^{-1}$ [30]. Concrete examples from the literature include porous lignin-derived carbons showing 420 F g^{-1} with

an SSA of 1660 $m^2 g^{-1}$ in alkaline electrolyte, which is clearly within the same performance range as commercial porous carbons used for charge storage [34]. More generally, activated lignin carbons commonly fall in the 500–2000 $m^2 g^{-1}$ range, with reported cases around 1850 $m^2 g^{-1}$, and have even been discussed as potential alternatives to commercial carbon black due to similarities in particle size and surface area [35].
However, "comparable" is not always sufficient, because many comparisons are still performed using powders, binder-based electrodes, and idealized geometries. In those cases, the lignin-derived carbon is not the electrode substrate itself, but only a component of a catalyst layer. As a result, key parameters such as mass transport, mechanical integrity, and in-plane conductivity are not properly evaluated at the substrate level.
From a sustainability perspective, fossil-based carbons mainly derived from PAN and pitch often involve energy-intensive processing. Cradle-to-gate LCA results reported for lignin-based carbon fibres show a climate impact of 1.50 kg CO_2-eq kg^{-1}, while a dataset for PAN-CF reports 38.9 kg CO_2-eq kg^{-1} in the current energy system (and 19.3 kg CO_2-eq kg^{-1} in a prospective cleaner energy system), which remains far higher than lignin-based fibres [36]. At the same time, these benefits depend strongly on the specific processing route and on the type and extraction of lignin, so the pathway must be clearly defined.
Overall, while some comparisons against fossil-based benchmarks exist, systematic studies that compare substrate versus substrate, employ free-standing architectures, and operate under realistic electrocatalytic conditions remain limited. This motivates the focus of the present thesis on lignin-derived free-standing mats and on direct benchmarking against commercial carbon papers.

1.6 Electrospun lignin-derived fibers and mats: state of the art

After discussing lignin-derived carbons in general terms, it is important to highlight that their properties strongly depend on the material architecture. Moving from powder-based materials to fibrous structures significantly changes the way transport occurs within an electrode, affects mechanical integrity, and modifies the role of the material itself when used as an electrode component. For this reason, architecture plays a central role in determining the final functionality of lignin-derived carbons.
Fibrous architectures, in particular, offer a continuous network for electronic transport, interconnected porosity, high specific surface area, and the possibility of being free-standing. These features make fibrous mats more comparable to conventional carbon papers and carbon cloths than to carbon powders. As a result, lignin-derived fibrous structures represent a promising platform for applications where both transport and mechanical stability are required.
Among the available processing techniques, electrospinning has emerged as a simple, versatile, and conceptually scalable approach to produce lignin-based fibers. This technique allows control over fiber diameter, enables the fabrication of continuous mats, and offers the possibility to incorporate additives by tuning the electrospinning parameters.
The present section therefore reviews the state of the art on lignin-derived fibers and mats, covering electrospinning of lignin-based solutions (1.6.1), stabilization and carbonization processes (1.6.2), resulting properties (1.6.3), and strategies to enhance mechanical and electrical performance (1.6.4).

1.6.1 Electrospinning of lignin and lignin-based polymer solutions

Electrospinning (Figure 10) of lignin is not trivial, meaning that the quality of the resulting fibers strongly depends on solution viscosity, electrical conductivity, and surface tension [3], [35]. If the viscosity is too low, bead formation or even electrospray is typically observed, whereas excessively high viscosities lead to solutions that are not spinnable.

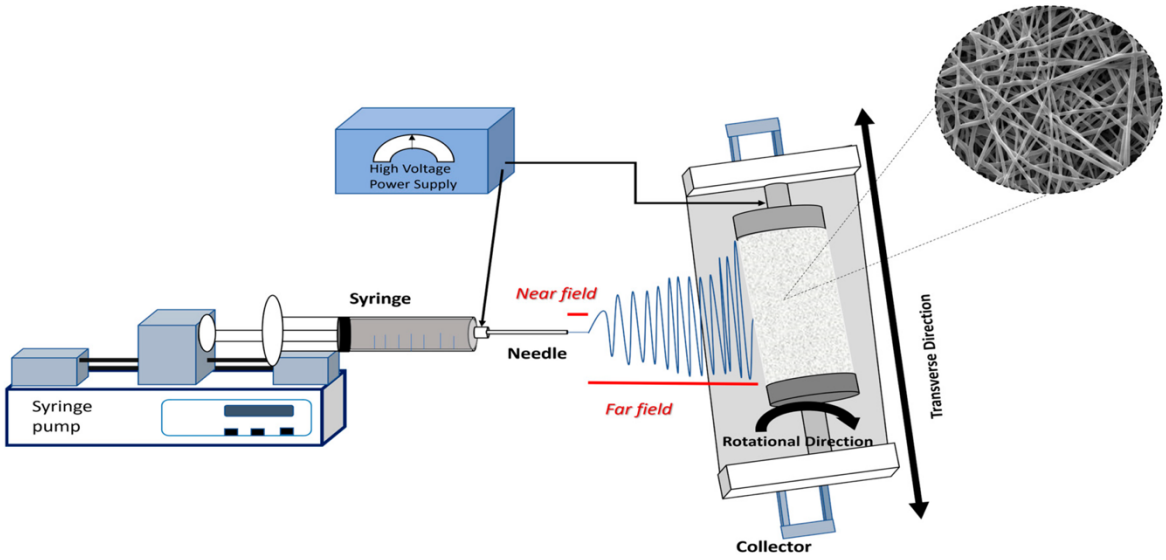

Figure 10 - Electrospinning setup. Reproduced from [41].

Lignin itself generally exhibits a relatively low molecular weight, which results in a limited number of chain entanglements; for this reason, lignin alone tends to produce electrospray or bead-on-string morphologies rather than continuous fibers [30], [35]. To overcome these intrinsic limitations, the use of processing aids is required, typically high-molecular-weight polymers such as polyethylene oxide (PEO), polyvinyl acetate (PVA), or polyacrylonitrile (PAN) in organic solvents [2], [35]. The introduction of carrier polymers should therefore not be regarded as an optional formulation choice, but rather as a process constraint necessary to enable electrospinning of lignin-based systems [3].
Based on the available literature, three main formulation routes can be identified to obtain electrospinnable lignin-based solutions [3], [35]. The first route involves the use of lignin alone by employing special electrospinning setups. A historical example is the processing of organosolv lignin without a binder polymer using coaxial or triaxial electrospinning, which enabled the formation of fibers with diameters on the order of 200 nm after stabilization and carbonization [35]. However, the most widely reported and practically relevant approach corresponds to the second route, based on blends of lignin with a water-soluble binder polymer such as PEO, PVA, or PAN. This is the most common strategy in the literature and also the one closest to the present thesis. PEO and PVA are frequently cited as relatively "green" carrier polymers, as they promote higher chain entanglement and lead to more uniform fiber morphologies [3], [37]. A classical example is the use of kraft lignin combined with PEO in DMF, followed by stabilization and carbonization. Another particularly relevant configuration involves organosolv lignin blended with PEO in alkaline aqueous solutions. Freshly prepared solutions of this type allow a high degree of chain entanglement and the formation of association-induced complexes, a feature that is especially relevant for the system investigated in this work [2], [3]. In this context, Poursorkhabi et al. showed that freshly prepared high-molecular-weight PEO solutions exhibit a non-equilibrium state characterized by a high degree of chain entanglement, which strongly affects flocculation behavior and solution stability. The extent of entanglement and flocculation was reported to depend on PEO molecular weight, solution history, shear conditions, and storage time, as well as on the presence of ions required for lignin dissolution in alkaline media. In lignin–PEO systems, the balance between PEO content and lignin concentration controls the formation of charged association complexes, which in turn influence solution spinnability and fiber formation. The third formulation route includes lignin-based systems combined with solvents, conditioning agents, or additives such as acids or salts. For example, the addition of phosphoric acid has been reported to increase solution conductivity and viscosity, modify fiber morphology toward more curly structures, and, in some cases, simplify or shorten the stabilization step [3], [30].

In addition to solution formulation, electrospinning process parameters play a key role in determining the final fiber morphology. Applied voltage, flow rate, tip-to-collector distance, and collector rotation speed directly influence fiber diameter and the presence of defects [3], [30]. The use of an appropriate solution concentration, and therefore viscosity, together with a high-molecular-weight carrier polymer such as high-Mw PEO, helps reduce bead formation and promotes the formation of uniform fibers [2], [3], [30], [35]. Typical operating conditions reported in the literature include applied voltages around 12 kV, tip-to-collector distances of 20–25 cm, and flow rates on the order of 1 mL h^{-1} [30]. By tuning both formulation and processing parameters, a wide range of morphologies can be obtained, including beaded fibers, straight fibers, fused meshes, and hollow or solid structures [3]. The morphology of the precursor mat has a direct impact on the subsequent stabilization and carbonization steps and therefore represents a key factor in determining the final properties of lignin-derived carbon fibers [2], [35].

1.6.2 Stabilization and carbonization of electrospun lignin fibers

After electrospinning, lignin fibers are polymeric and organic in nature, they are not yet carbon materials and, most importantly, they are not thermally stable. When as-spun lignin fibers are directly heated to high temperatures under inert atmosphere, such as nitrogen or argon, they tend to soften and undergo fiber fusion, leading to the merging of adjacent fibers. As a consequence, the porous network can collapse and the fibrous mat architecture may be lost [3], [37], [38].For this reason, prior to carbonization, it is necessary to fix the fiber morphology at lower temperatures in order to avoid such structural degradation. The main objective of stabilization is to render the fibers infusible by inducing crosslinking and condensation reactions, which reduce molecular mobility and increase the thermal integrity of the fibrous network [35], [38]. Stabilization is typically carried out in air at moderate temperatures, generally in the range of 200–300 °C, using low heating rates (often around 1 °C min^{-1}), promoting oxidation, dehydration, and condensation reactions within the lignin structure [3], [37]. The stabilization protocol strongly depends on several factors, including the type of lignin, the presence and amount of carrier polymer in the electrospinning solution, and the fiber diameter. Improper stabilization conditions may result in excessive mass loss due to the release of volatile species, pronounced fiber shrinkage, and increased brittleness of the resulting carbon network. As a result, stabilization strategies reported in the literature vary significantly with lignin source, solution composition, and electrospun fiber morphology [3], [35]. In some specific systems, particularly lignin–polyethylene oxide formulations prepared in alkaline media such as sodium hydroxide solutions, strong intermolecular interactions, associations, and ion-mediated complexes have been reported. These interactions can promote partial condensation and crosslinking already before thermal treatment, enhancing the thermal integrity of the fibers [2], [22], [38]. Under such conditions, the stabilization step can be shortened or made less severe and, in some cases, replaced by simplified thermal treatments, where stabilization progressively occurs during a slow heating ramp under inert atmosphere rather than through a dedicated oxidative step [37], [38].

After stabilization, the fibers are subjected to carbonization at high temperatures under inert atmosphere, typically between 800 and 1200 °C, in order to convert the organic matrix into aromatic carbon structures [30], [35]. Increasing the carbonization temperature generally leads to a higher degree of aromatization, a reduction of oxygen-containing functional groups, and an increase in electrical conductivity, while the resulting carbon structure remains predominantly turbostratic rather than graphitic [30], [39].

During carbonization, a significant mass loss and fiber shrinkage occur, accompanied by the development of internal stresses. These effects can result in increased brittleness, mechanically weak mats, and a higher susceptibility to fracture, particularly in free-standing architectures [35], [39]. Carbonization therefore introduces an intrinsic trade-off between porosity and surface area, electrical conductivity, and mechanical integrity, which becomes especially critical for free-standing carbon mats designed to act as electrode substrates. For this reason, several studies have explored reinforcement strategies, including the incorporation of conductive fillers such as carbon nanotubes, to improve the combined electrical and mechanical performance of lignin-derived carbon mats [2], [39].

1.6.3 Properties and applications of lignin-based electrospun carbon fibers

After stabilization and carbonization, lignin-derived electrospun carbon fibers typically exhibit electrical conductivity, interconnected porosity, high specific surface area, and a surface chemistry that can be either rich or depleted in functional groups, depending on strongly tunable parameters such as carbonization temperature, lignin type, and the presence of carrier polymers or additives [2], [30], [35]. These properties can be tailored over a wide range, making lignin-derived fibers attractive for several electrochemical applications reported in the literature.

Most of the reported applications of lignin-based electrospun carbons are related to energy storage technologies, such as supercapacitors and batteries, as well as to electrocatalytic reactions including oxygen reduction and oxygen evolution reactions [1], [2], [30]. In many of these studies, the electrospun fibers are either ground into powders or employed as binder-based electrodes, where the carbon material acts as the active phase dispersed within a catalytic or conductive layer. As a result, even when high electrochemical performance is achieved, the carbon material is not evaluated as an electrode substrate, but rather as a component of a composite electrode layer [2], [3].

This approach introduces clear structural limitations. Key properties that are essential for electrode substrates, such as in-plane electrical conductivity, long-term mechanical integrity, and continuous mass transport through a three-dimensional porous network, are rarely assessed in the literature [3], [9]. Although free-standing lignin-derived fibrous architectures have been reported, they are predominantly designed for energy storage applications and are not specifically engineered to replace conventional carbon paper or carbon cloth substrates used in electrochemical devices [2], [35].

One of the most recurrent limitations of lignin-derived fibers and mats is their intrinsic fragility and the trade-off between high porosity and mechanical strength. This challenge has motivated the development of various reinforcement strategies, including polymer blending and the incorporation of conductive fillers such as carbon nanotubes, aimed at improving the combined mechanical and electrical performance of lignin-derived electrospun carbon mats [2], [39].

1.6.4 Strategies to enhance mechanical and electrical properties (MWCNT)

Despite their promising electrochemical properties, lignin-derived electrospun fibers and mats are often intrinsically fragile, exhibit low mechanical strength, and suffer from a trade-off between porosity and robustness. These limitations restrict their handling, their use as free-standing substrates, and their long-term stability under operating conditions. As a result, lignin-based fibrous carbons are frequently characterized by brittleness, limited mechanical integrity, and poor resistance to mechanical stress [2], [35], [39].

One effective strategy to mitigate these issues is the incorporation of carbon nanotubes (CNTs). CNTs are widely used due to their high aspect ratio, excellent electrical conductivity, and good compatibility with carbonaceous matrices. In lignin-based systems, CNTs can enhance electronic transport by providing additional conductive pathways, act as reinforcement bridges between adjacent fibers, and reduce crack initiation and propagation within the fibrous network [2], [39]. In particular, oxidized carbon nanotubes are often preferred, as surface oxygen-containing functional groups improve their dispersion and promote stronger interactions with lignin and polyethylene oxide in the electrospinning solution [3].

However, despite these advantages, only a limited number of studies have explored the incorporation of CNTs into electrospun lignin-based mats and their role is most often investigated in binder-based electrodes or composite powders rather than in free-standing architectures. Moreover, CNT-reinforced lignin mats are seldom evaluated as electrode substrates or directly compared with commercial carbon paper benchmarks. Finally, systematic studies correlating CNT dispersion with mechanical properties, or assessing the impact of CNT incorporation on electrochemical performance in liquid-phase electrocatalytic reactions, remain largely missing in the current literature [3], [39], [40].

1.7 Research gap: towards lignin-derived electrospun carbon mats as electrode substrates

The available literature on lignin-derived carbon materials is extensive but not convergent. While these materials have been widely investigated, they are typically studied for very different objectives, which makes the reported results difficult to compare in the context of the application addressed in this thesis. The main limitation therefore does not lie in the material itself, but rather in the way it has been evaluated. Most studies assess lignin-derived carbons as powders, active materials, or catalyst supports, rather than as electrode substrates. As a result, a substrate-centric evaluation is still largely missing (Figure 11). Consequently, it remains unclear whether lignin-derived carbon architectures can move beyond laboratory-scale demonstrations and function as practical electrode substrates comparable to commercial carbon papers.

Key substrate-related properties such as in-plane electrical conductivity, mechanical integrity, and continuous mass transport through the porous network do not emerge from binder-based electrode configurations or from idealized electrochemical setups such as rotating disk electrodes or conventional H-cell geometries. Without addressing these aspects, it remains unclear whether lignin-based architectures are merely promising materials or can realistically replace conventional fossil-derived substrates. A direct comparison with established benchmarks such as carbon paper and carbon cloth is therefore required to properly assess their practical relevance.

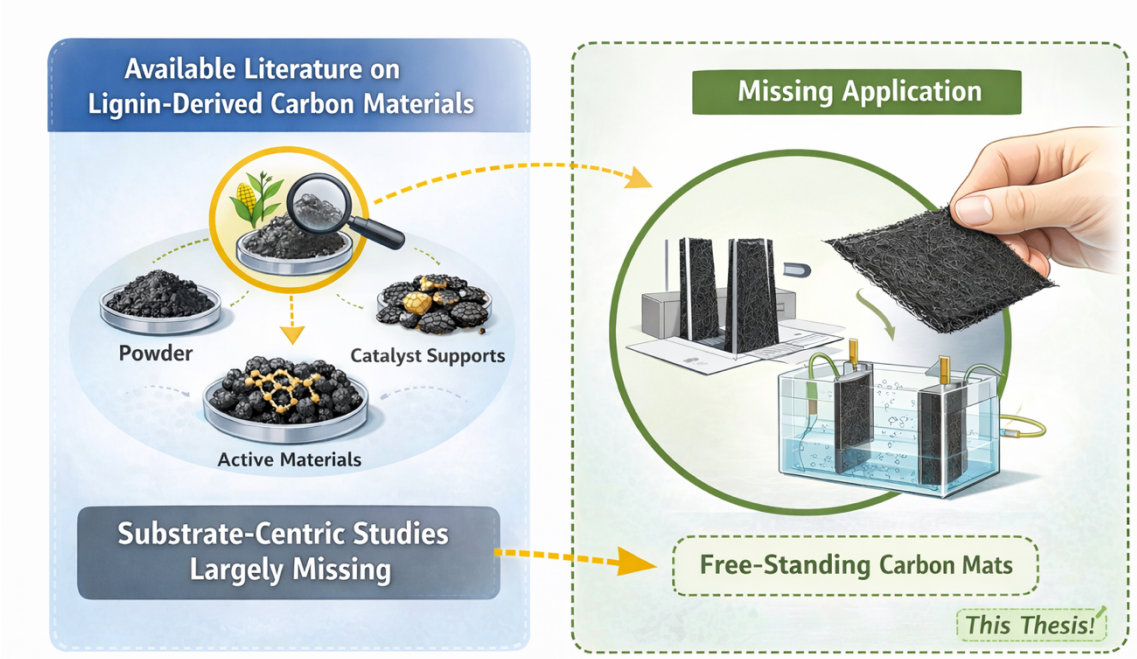

Figure 11 - Schematic representation of the literature landscape on lignin-derived carbon materials and the research gap addressed in this thesis, focusing on their evaluation as free-standing electrode substrates. Illustration by author.

This thesis addresses this gap by designing lignin-derived electrospun carbon mats as free-standing electrode substrates and by evaluating their morphology, structural integrity, and electrochemical behavior under realistic operating conditions, using biomass electro-oxidation as a representative case study.

1.8 Abstract

Carbon-based electrode substrates are key components in electrochemical systems, yet they are almost exclusively derived from fossil resources, which contrasts with sustainability and circular economy principles. In this work, lignin is investigated as a renewable precursor for the fabrication of free-standing carbon electrode substrates. Lignin-based solutions are processed by electrospinning to obtain fibrous mats, which are subsequently converted into carbon through thermal treatment. The incorporation of oxidized carbon nanotubes is explored as a strategy to tune the structural and electrochemical performance of the resulting lignin-derived mats. The materials are characterized in terms of morphology, porosity, surface chemistry, and structural order. Their performance as electrode substrates is evaluated under realistic electrochemical conditions using the glycerol oxidation reaction (GOR) as a representative biomass-derived anodic process and directly compared with a commercial fossil-derived carbon paper at identical catalyst loading. The results show that lignin-derived electrospun carbon mats can achieve electrochemical performances comparable to conventional carbon substrates while offering advantages in terms of renewable origin and processing flexibility. At the same time, current limitations related to structural optimization are identified. Overall, this work highlights the potential of lignin-derived free-standing carbon mats as sustainable alternatives to fossil-based electrode substrates in electrocatalytic systems.

References

[1] E. Antolini, 'Lignocellulose, Cellulose and Lignin as Renewable Alternative Fuels for Direct Biomass Fuel Cells', Jan. 07, 2021, *Wiley-VCH Verlag*. doi: 10.1002/cssc.202001807.

[2] X. Wu *et al.*, 'Lignin-derived electrochemical energy materials and systems', May 01, 2020, *John Wiley and Sons Ltd*. doi: 10.1002/bbb.2083.

[3] F. J. García-Mateos, R. Ruiz-Rosas, J. M. Rosas, J. Rodríguez-Mirasol, and T. Cordero, 'Controlling the composition, morphology, porosity, and surface chemistry of lignin-based electrospun carbon materials', Apr. 15, 2019, *Frontiers Media S.A.* doi: 10.3389/fmats.2019.00114.

[4] L. Dessbesell, M. Paleologou, M. Leitch, R. Pulkki, and C. (Charles) Xu, 'Global lignin supply overview and kraft lignin potential as an alternative for petroleum-based polymers', *Renewable and Sustainable Energy Reviews*, vol. 123, no. 10, p. 109768, May 2020, doi: 10.1016/j.rser.2020.109768.

[5] X. Huang *et al.*, 'Preparation, performance enhancement, and energy storage applications of lignin-based carbon nanofibers', Feb. 01, 2025, *Springer Science and Business Media Deutschland GmbH*. doi: 10.1007/s13399-024-05387-7.

[6] E. Svinterikos, I. Zuburtikudis, and M. Al-Marzouqi, 'Electrospun Lignin-Derived Carbon Micro- And Nanofibers: A Review on Precursors, Properties, and Applications', Sep. 21, 2020, *American Chemical Society*. doi: 10.1021/acssuschemeng.0c03246.

[7] T. Wang, Z. Liu, P. Li, H. Wei, K. Wei, and X. Chen, 'Lignin-derived carbon aerogels with high surface area for supercapacitor applications', *Chemical Engineering Journal*, vol. 466, Jun. 2023, doi: 10.1016/j.cej.2023.143118.

[8] J. Ralph, C. Lapierre, and W. Boerjan, 'Lignin structure and its engineering', Apr. 01, 2019, *Elsevier Ltd*. doi: 10.1016/j.copbio.2019.02.019.

[9] S. Park, J. W. Lee, and B. N. Popov, 'A review of gas diffusion layer in PEM fuel cells: Materials and designs', 2012, *Elsevier Ltd*. doi: 10.1016/j.ijhydene.2011.12.148.

[10] G. Dodekatos, S. Schünemann, and H. Tüysüz, 'Recent Advances in Thermo-, Photo-, and Electrocatalytic Glycerol Oxidation', Jul. 06, 2018, *American Chemical Society*. doi: 10.1021/acscatal.8b01317.

[11] L. Fan, B. Liu, X. Liu, N. Senthilkumar, G. Wang, and Z. Wen, 'Recent Progress in Electrocatalytic Glycerol Oxidation', Feb. 01, 2021, *Wiley-VCH Verlag*. doi: 10.1002/ente.202000804.

[12] A. Ben Abderrahmane, S. Tingry, D. Cornu, and Y. Holade, 'Progress in Biomass Electro-Valorization for Paired Electrosynthesis of Valuable Chemicals and Fuels', Aug. 01, 2024, *John Wiley and Sons Inc*. doi: 10.1002/aesr.202300302.
[13] H. Ye *et al.*, 'Progress and Challenges in Electrochemical Glycerol Oxidation: The Importance of Benchmark Methods and Protocols', *ChemCatChem*, vol. 17, no. 13, Jul. 2025, doi: 10.1002/cctc.202500152.
[14] IPCC, 'Climate Change 2023: Synthesis Report', Geneva, 2023.
[15] IEA, 'World Energy Outlook', Paris, France, 2025.
[16] J. Liu, J. Yang, Y. Dou, X. Liu, S. Chen, and D. Wang, 'Deactivation Mechanism and Mitigation Strategies of Single-Atom Site Electrocatalysts', *Advanced Materials*, vol. 37, no. 27, Jul. 2025, doi: 10.1002/adma.202420383.
[17] X. Zhang, Y. Liu, X. Ma, X. Liu, R. Zhang, and Y. Wang, 'Metal–Support Interaction of Carbon–Based Electrocatalysts for Oxygen Evolution Reaction', *Nanoenergy Advances 2023, Vol. 3, Pages 48-72*, vol. 3, no. 1, pp. 48–72, Mar. 2023, doi: 10.3390/nanoenergyadv3010004.
[18] X. Hu, J. Lu, Y. Liu, L. Chen, X. Zhang, and H. Wang, 'Sustainable catalytic oxidation of glycerol: a review', Oct. 01, 2023, *Springer Science and Business Media Deutschland GmbH*. doi: 10.1007/s10311-023-01608-z.
[19] B. Caglar, Y. El Hassan, O. Basak, and A. Hepbasli, 'Electrooxidation of Glycerol on Monometallic and Bimetallic Catalysts-Containing Porous Carbon Cloth Electrodes in an Alkaline Medium', *J. Electrochem. Soc.*, vol. 168, no. 8, p. 084506, Aug. 2021, doi: 10.1149/1945-7111/ac1a57.
[20] C. A. Angelucci, J. Souza-Garcia, P. S. Fernández, P. V. B. Santiago, and R. M. L. M. Sandrini, 'Glycerol Electrooxidation on Noble Metal Electrode Surfaces', *Encyclopedia of Interfacial Chemistry: Surface Science and Electrochemistry*, pp. 643–650, Jan. 2018, doi: 10.1016/B978-0-12-409547-2.13330-X.
[21] A. Jayakumar, S. Singamneni, M. Ramos, A. M. Al-Jumaily, and S. S. Pethaiah, 'Manufacturing the Gas Diffusion Layer for PEM Fuel Cell Using a Novel 3D Printing Technique and Critical Assessment of the Challenges Encountered', *Materials 2017, Vol. 10,* vol. 10, no. 7, Jul. 2017, doi: 10.3390/ma10070796.
[22] V. Poursorkhabi, M. A. Abdelwahab, M. Misra, H. Khalil, B. Gharabaghi, and A. K. Mohanty, 'Processing, Carbonization, and Characterization of Lignin Based Electrospun Carbon Fibers: A Review', Sep. 09, 2020, *Frontiers Media S.A.* doi: 10.3389/fenrg.2020.00208.
[23] M. Ramesh, L. Rajeshkumar, and R. Bhoopathi, 'Carbon substrates: a review on fabrication, properties and applications', Aug. 01, 2021, *Springer*. doi: 10.1007/s42823-021-00264-z.
[24] M. Zhang, M. Yang, M. Yaguchi, H. Jintoku, S. Sakurai, and D. Futaba, 'Understanding and controlling the oxidation degree of single-wall carbon nanotubes: A comparative study of treatment processes', *Carbon N. Y.*, vol. 237, p. 120132, Apr. 2025, doi: 10.1016/j.carbon.2025.120132.
[25] S. Mateo, G. Fabbrizi, and A. J. Moya, 'Lignin from Plant-Based Agro-Industrial Biowastes: From Extraction to Sustainable Applications', *Polymers 2025, Vol. 17,* vol. 17, no. 7, Mar. 2025, doi: 10.3390/polym17070952.
[26] X. Shi, X. Wang, B. Tang, Z. Dai, K. Chen, and J. Zhou, 'Impact of lignin extraction methods on microstructure and mechanical properties of lignin-based carbon fibers', *J. Appl. Polym. Sci.*, vol. 135, no. 10, Mar. 2018, doi: 10.1002/app.45580.
[27] M. Margarida Martins, F. Carvalheiro, and F. Gírio, 'An overview of lignin pathways of valorization: from isolation to refining and conversion into value-added products', *Biomass Convers. Biorefin.*, vol. 14, no. 3, pp. 3183–3207, Feb. 2024, doi: 10.1007/s13399-022-02701-z.
[28] A. Beaucamp, M. Muddasar, T. Crawford, M. N. Collins, and M. Culebras, 'Sustainable lignin precursors for tailored porous carbon-based supercapacitor electrodes', *Int. J. Biol. Macromol.*, vol. 221, pp. 1142–1149, Nov. 2022, doi: 10.1016/j.ijbiomac.2022.09.097.

[29] P. Schlee *et al.*, 'From Waste to Wealth: From Kraft Lignin to Free-standing Supercapacitors', *Carbon N. Y.*, vol. 145, no. 1–2, pp. 470–480, Apr. 2019, doi: 10.1016/j.carbon.2019.01.035.
[30] W. Zhang *et al.*, 'Lignin Derived Porous Carbons: Synthesis Methods and Supercapacitor Applications', Nov. 01, 2021, *John Wiley and Sons Inc*. doi: 10.1002/smtd.202100896.
[31] F. Meng *et al.*, 'Carbon-based metal-free catalysts for selective oxidation of glycerol to glycolic acid', *Chem. Eng. Sci.*, vol. 268, Mar. 2023, doi: 10.1016/j.ces.2022.118394.
[32] H. Ji *et al.*, 'Capacitance of carbon-based electrical double-layer capacitors', *Nat. Commun.*, vol. 5, Feb. 2014, doi: 10.1038/ncomms4317.
[33] V. D. Obasa *et al.*, 'A Review on Lignin-Based Carbon Fibres for Carbon Footprint Reduction', *Atmosphere 2022, Vol. 13*, vol. 13, no. 10, Sep. 2022, doi: 10.3390/atmos13101605.
[34] P. Zhao *et al.*, 'Highly Active N, S Codoped Porous Carbon Derived from Lignin-Rich Pulping Waste Liquor for Supercapacitors and Oxygen Reduction Reaction', *Energy and Fuels*, vol. 38, no. 4, pp. 3159–3170, Feb. 2024, doi: 10.1021/acs.energyfuels.3c03915.
[35] S. Chatterjee and T. Monori Saito, 'Lignin-Derived Advanced Carbon Materials', doi: 10.1002/cssc.201500692.
[36] M. Janssen, E. Gustafsson, L. Echardt, J. Wallinder, J. Wolf, and S. Skogsägarna ekonomisk förening, 'Life cycle assessment of lignin-based carbon fibres', 2019, Accessed: Mar. 13, 2026. [Online]. Available: https://urn.kb.se/resolve?urn=urn:nbn:se:ri:diva-40763
[37] M. Kumar, M. Hietala, and K. Oksman, 'Lignin-based electrospun carbon nanofibers', Apr. 15, 2019, *Frontiers Media S.A.* doi: 10.3389/fmats.2019.00062.
[38] M. Cho, M. Karaaslan, S. Chowdhury, F. Ko, and S. Renneckar, 'Skipping Oxidative Thermal Stabilization for Lignin-Based Carbon Nanofibers', *ACS Sustain. Chem. Eng.*, vol. 6, no. 5, pp. 6434–6444, May 2018, doi: 10.1021/acssuschemeng.8b00209.
[39] J. Chen, T. Ghosh, T. Tang, and C. Ayranci, 'Optimization of high-quality carbon fiber production from electrospun aligned lignin fibers', *Polym. Eng. Sci.*, vol. 62, no. 4, pp. 1256–1268, Apr. 2022, doi: 10.1002/pen.25923.
[40] S. Wang *et al.*, 'Reinforcement of lignin-based carbon fibers with functionalized carbon nanotubes', *Compos. Sci. Technol.*, vol. 128, no. 6, pp. 116–122, May 2016, doi: 10.1016/j.compscitech.2016.03.018.
[41] M. Ahmadi Bonakdar and D. Rodrigue, "Electrospinning: Processes, Structures, and Materials," *Macromol 2024, Vol. 4, Pages 58-103*, vol. 4, no. 1, pp. 58–103, Feb. 2024, doi: 10.3390/macromol4010004.

2 Chapter 2 – Materials and Methods

2.1 Raw materials

2.1.1 Organosolv lignin

Organosolv lignin was used as received in powder form. The lignin was supplied by Fraunhofer and employed without further purification.

2.1.2 Polymer carrier (PEO) and NaOH aqueous solution

Polyethylene oxide (PEO, Mw = 400'000 g mol^{-1}) was used as polymer carrier. Sodium hydroxide pellets were dissolved in deionized water to prepare alkaline solutions.

2.1.3 Multi-walled carbon nanotubes (MWCNTs) and oxidation reagents

Multi-walled carbon nanotubes (MWCNTs) were supplied by canrd. Oxidized MWCNTs were obtained as described in Section 2.2.3. As oxidation reagents, sulphuric acid 98% and nitric acid 65% were used.

2.1.4 Pt/C catalyst and ionomers (Nafion + Sustainion XA 9)

A commercial Pt/C catalyst (60 wt% Pt) was used for catalyst deposition. Nafion and Sustainion XA-9 ionomers were employed for ink preparation.

2.1.5 Commercial fossil-derived carbon substrate used as benchmark

A commercial carbon paper (Freudenberg H23) was used as fossil-derived benchmark substrate for electrocatalysis.

2.2 Preparation of electrospinning solutions

Electrospinning solutions were prepared starting from lignin-based formulations using a polymer carrier and alkaline aqueous media. Different formulations were employed to investigate the effect of solution composition on fiber formation and final mat properties.

2.2.1 Lignin–PEO–NaOH base solution

The lignin-PEO-NaOH base solution is composed of 1.2 g of lignin, 0.15 g of PEO and 7.8 g of NaOH 0.5 M solution. To make such solution, on the first day PEO is added to the NaOH solution and stirred overnight. On the next day, lignin is also added and stirred overnight before the day of electrospinning.

2.2.2 Oxidation of MWCNTs and incorporation in solution (0.5–0.75 wt%)

Multi-walled carbon nanotubes (MWCNTs) were oxidized via acid treatment to improve their dispersibility in aqueous alkaline media [1], [2]. A mixture of concentrated sulfuric acid and nitric acid (3:1 v/v) was prepared under cooling, and the MWCNTs were added under stirring. The suspension was treated under controlled temperature (40 °C) to promote surface oxidation [3], [4]. The reaction was quenched by dilution with deionized water, and the oxidized MWCNTs were recovered by vacuum filtration. The solid was extensively washed with deionized water until neutral pH was reached and subsequently redispersed in aqueous sodium hydroxide solution to obtain a stock dispersion of known concentration, which was 4.75 mg/mL. The solution shows homogenous dispersion of CNTs, as shown in Figure 12.

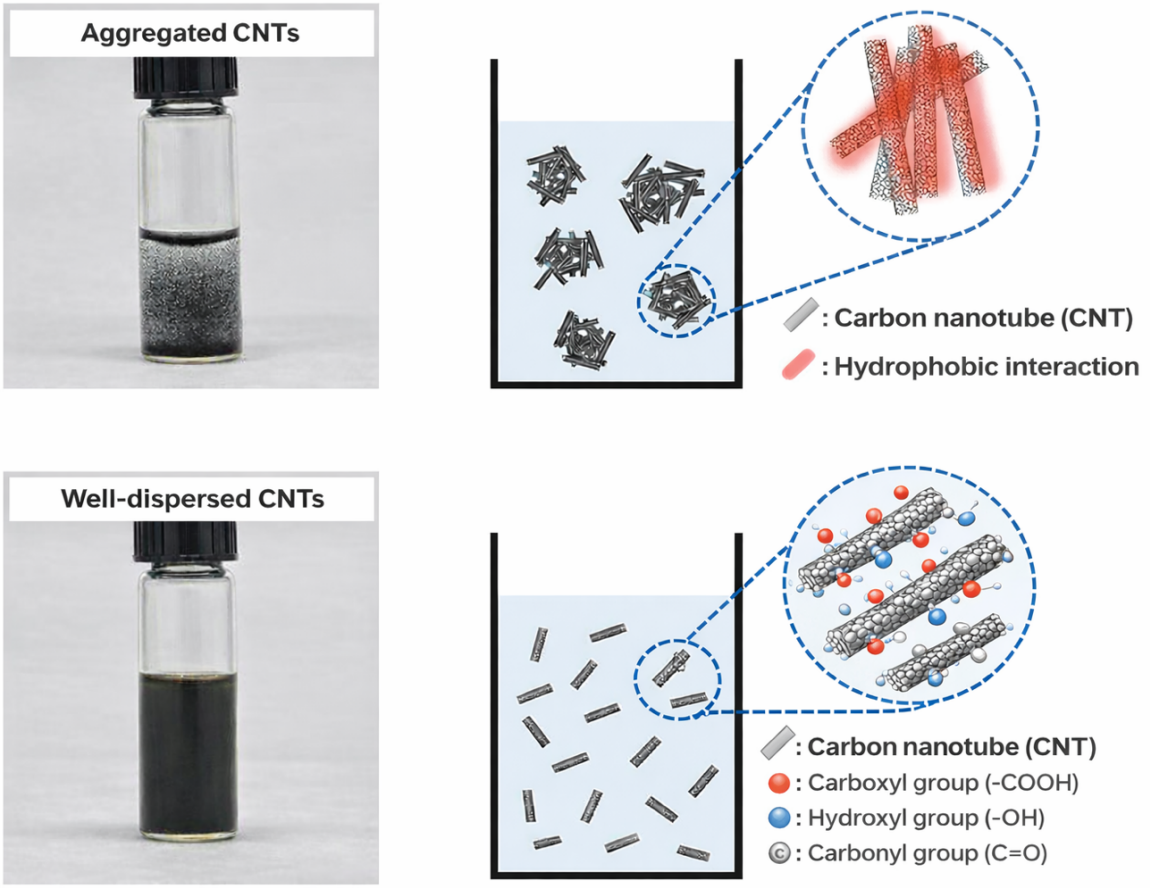

Figure 12 - Effect of oxidation of MWCNTs. Adapted from [5]

2.2.3 Incorporation of oxidized MWCNTs in electrospinning solutions (0.5-0.75 wt%)

Electrospinning solutions were prepared using an aqueous sodium hydroxide solution (0.5 M) as solvent. On the first day, polyethylene oxide (PEO) was dissolved in the alkaline solution under magnetic stirring and left to mix overnight to ensure complete dissolution. On the second day, a predefined volume of the oxidized MWCNT aqueous dispersion was added to the PEO/NaOH solution to achieve the desired CNT weight fraction. The mixture was stirred until an optically homogeneous dispersion was obtained. Subsequently, lignin powder was gradually added to the solution and the suspension was left under continuous stirring overnight to allow for complete lignin dissolution and homogeneous distribution of all components.

2.3 Electrospinning process

Electrospinning was employed to fabricate lignin-based fibrous mats starting from the prepared polymer solutions. The process parameters and collection strategy were controlled to obtain continuous, self-supported nonwoven mats suitable for subsequent thermal treatment.

2.3.1 Electrospinning setup, operating parameters and summary of all electrospun samples

Electrospinning was carried out using a laboratory-scale electrospinning setup consisting of a high-voltage power supply, a syringe pump, and a grounded collector. The polymer solutions were loaded into plastic syringes and delivered through a metallic needle at a controlled flow rate using a syringe pump. A high voltage was applied between the needle and the collector to generate a stable polymer jet and induce fiber formation.
The distance between the needle tip and the collector, the applied voltage, and the solution flow rate were systematically controlled to ensure stable electrospinning conditions and

reproducible fiber morphologies. A rotating drum collector, covered with aluminum foil, was employed to obtain continuous fibrous mats with a self-supported nonwoven structure.
All electrospinning experiments were performed inside a humidity-controlled enclosure, with the relative humidity maintained at approximately 25%. Electrospinning was conducted at ambient temperature. The operating parameters used for each formulation are summarized in Table 2.

Table 2 – Summary table of all samples and their electrospinning parameters

Sample ID	Lignin (g)	PEO (g)	NaOH 0.5M (g)	Ox-MWCNT (wt% vs lignin and PEO)	Voltage (kV)	Flow rate (mL/h)	Distance (cm)
LDM	1.20	0.15	7.8	0	20	2	20
LDM-0.5CNT	1.20	0.20	7.8	0.5	20	1.6	20
LDM-0.75CNT	1.25	0.20	7.8	0.75	20	1.5	20

The amounts of lignin and PEO added to the formulations was increased in the CNT enriched ones to match the addition of solvent from the oxidized MWCNT 4.75 mg/mL alkaline solution, so that processability wouldn't be affected. Therefore, flow rates were decreased to avoid spitting during the electrospinning process. Lastly, CNT contents are reported relative to the as-prepared electrospinning formulation. Due to mass loss during carbonization, the effective CNT fraction in the final carbon mat is higher, as shown in 2.4.1.

2.3.2 Fabrication of base and CNT-reinforced lignin mats

After completion of the electrospinning process, the relative humidity inside the controlled enclosure was gradually returned to ambient conditions. Once the relative humidity reached approximately 30–35%, the electrospinning chamber was opened and the rotating drum collector was removed. The aluminium foil used as collecting substrate was carefully detached from the collector and laid flat.

The electrospun fibrous mat was then cut into strips of the desired dimensions and gently peeled off from the original aluminium foil. Each mat was subsequently transferred onto a fresh aluminium foil support to facilitate handling and avoid damage to the fibrous structure. The samples were finally wrapped in aluminium foil, allowing multiple specimens to be stored together.

Prior to thermal treatment, the electrospun mats were either stored under vacuum at 80 °C or directly transferred to the furnace for carbonization.

2.4 Thermal treatments

Thermal treatments were applied to the electrospun lignin-based mats to stabilize the fibrous morphology and convert the organic precursor into carbon materials. Different thermal steps were adopted depending on the formulation and processing route.

2.4.1 Carbonization in N_2

Carbonization of the electrospun mats was performed in a horizontal tube furnace (MTI Corporation, USA) under a continuous nitrogen flow. The samples were placed in the furnace and heated under a continuous flow of nitrogen to prevent oxidation during thermal treatment.

The temperature was increased from room temperature to the target carbonization temperature using a controlled heating rate of one degree per minute, followed by an

isothermal dwell at the final temperature. After carbonization, the furnace was allowed to cool down naturally to room temperature under nitrogen flow before sample removal.
This thermal treatment converted the organic electrospun fibers into carbonaceous fibrous mats while preserving the overall nonwoven architecture. The samples were carbonized under an inert atmosphere by heating from room temperature to the target temperature at a ramp rate of 1 °C min^{-1}, followed by a 2 h dwell at the peak temperature, and subsequently allowed to cool naturally to room temperature.

Based on literature reports, lignin-derived electrospun mats typically exhibit a carbon yield of approximately 36% after carbonization under similar thermal conditions [6]. Assuming a comparable yield in the present work, a mass balance estimation was performed to approximate the effective CNT fraction in the final carbonized mats, with resulting updated concentrations in Table 3.

Table 3 - CNT concentration in formulations before electrospinning and in final fibers after carbonization. Assuming 36% C wield for organosolv lignin [6]

Sample ID	Formulation CNT loading (wt%)	Post carbonization CNT concentration (wt%)
LDM-0.5CNT	0.5	~1.4
LDM-0.75CNT	0.75	~2.2

Since the polymeric components undergo significant mass loss during carbonization while CNTs remain largely preserved, the relative CNT content in the final carbon structure is expected to increase compared to the initial formulation. The values reported are therefore theoretical estimates based on literature yield data and should be interpreted accordingly.

2.5 Post-treatment and catalyst deposition

After carbonization, the lignin-derived carbon mats were subjected to post-treatment steps and catalyst deposition prior to electrochemical testing. These procedures were applied to both lignin-based mats and commercial benchmark substrates to ensure comparability.

2.5.1 Acid washing in HCl 0.5 M and DI water

After carbonization, the lignin-derived carbon mats were subjected to an acid washing treatment to remove residual inorganic species and soluble impurities originating from the precursor formulation and thermal processing. The samples were immersed in an aqueous hydrochloric acid solution (0.5 M) and left undisturbed for 45 minutes.

After acid treatment, the mats were thoroughly rinsed with deionized water until neutral pH was reached. The washed samples were then prepared for subsequent drying and post-treatment steps.

2.5.2 Drying (EtOH + 80 °C overnight)

After acid washing, the carbon mats were briefly wetted with ethanol to facilitate subsequent drying and prevent adhesion to solid surfaces. The samples were then placed in glass Petri dishes and covered with perforated aluminium foil to allow solvent evaporation while minimizing mechanical disturbance.
Drying was carried out at 80 °C until complete solvent removal. After drying, the mats could be easily detached from the Petri dishes without damage and were ready for further processing.

2.5.3 Preparation of Pt/C inks and manual spray coating

Catalyst inks were prepared by dispersing a commercial Pt/C catalyst in a mixed solvent system. The catalyst ink used for spray coating was prepared by mixing 4200 μL of

deionized water, 1584 μL of ethanol, and 216 μL of binder (either Nafion or Sustainion XA-9). The ionomer was added to the ink to promote adhesion of the catalyst layer to the carbon substrate. For most samples, Nafion was used as ionomer in the catalyst ink. In some cases, Sustainion XA-9 was used as an alternative ionomer. The ink formulations were otherwise kept identical. The suspension was probe sonicated for a fixed period to obtain a homogeneous and stable dispersion prior to deposition. The catalyst ink was then deposited onto the carbon substrates by manual spray coating. Both lignin-derived carbon mats and the commercial carbon paper were coated using the same ink formulation and deposition procedure to ensure direct comparability between samples.

2.5.4 Target Pt loading (0.19 mg_{Pt} cm^{-2}) on lignin-derived mats and benchmark substrate

The catalyst loading was controlled by adjusting the amount of ink deposited during spray coating on a heated surface at 35 °C, to promote solvent evaporation. A target platinum loading of 0.19 mg_{Pt} cm^{-2} was applied to all samples. This loading was selected after SEM evaluation and comparison with electrodes prepared with approximately twice the catalyst loading. The higher loading produced a carpet-like structure on the carbon nanofibers, so the lower loading was chosen as a standard for this work.
The same loading and deposition protocol were used for lignin-derived mats and for the commercial fossil-derived carbon paper to enable a direct comparison between substrates. To reach such target, the mats were regularly weighted after solvent evaporation during manual spray-coating.
After deposition, the coated electrodes were allowed to dry under ambient conditions before electrochemical testing.

2.6 Electrochemical measurements

Electrochemical measurements were performed using a Bio-Logic VMP-300 multichannel potentiostat/galvanostat (Bio-Logic Science Instruments, France). Electrochemical measurements were performed to evaluate the behavior of the prepared electrodes under conditions relevant to biomass electro-oxidation. All measurements were carried out using a standard three-electrode configuration.

2.6.1 CV data acquisition and analysis for GOR

Cyclic voltammetry was used to study the electrochemical behaviour of the prepared electrodes and to evaluate their activity toward glycerol electro-oxidation. Measurements were carried out in alkaline electrolyte, both in the absence and in the presence of glycerol, in order to separate the background response of the electrode from the contribution of glycerol oxidation.
CVs were recorded within a defined potential window at a fixed scan rate. Before recording the glycerol-containing measurements, several conditioning cycles were applied to stabilize the electrode response. For comparison, background voltammograms were collected in the same electrolyte without glycerol under identical conditions.
All CV measurements were performed at room temperature, submerging 1 cm^2 of each sample and of the counter electrode (CE) in the electrolyte. The potential window ranged from −0.9 V to 0.1 V vs. Hg/HgO (reference electrode) and was subsequently converted to the reference hydrogen electrode (RHE) scale for clearer comparison with literature data. A total of 50 cycles was recorded for each measurement. A platinum wire was used as the counter electrode.

2.6.2 Electrolyte composition for glycerol electro-oxidation

The electrolyte used for electrochemical measurements consisted of an aqueous alkaline solution prepared by dissolving sodium hydroxide (NaOH, Suprapur grade, Suprapur®, Merck) in deionized water. A 1 M NaOH solution was used as the background electrolyte for reference measurements.

For glycerol electro-oxidation experiments, glycerol was added to the alkaline solution to obtain a final composition of 1 M NaOH and 1 M glycerol. Fresh electrolyte solutions were prepared prior to each set of measurements to ensure reproducibility.

2.7 Fiber mat characterization

The lignin-derived fibrous mats were characterized using a combination of morphological, structural, textural, and electrochemical techniques to assess their suitability as electrode substrates.

2.7.1 SEM imaging of carbonized lignin-based mats

Scanning electron microscopy (SEM) was used to investigate the morphology of the electrospun mats after carbonization, spray-coating and catalysis. SEM images were acquired using a Zeiss GeminiSEM field-emission scanning electron microscope (Carl Zeiss AG, Germany) to evaluate fiber diameter, fiber uniformity, and the overall structure of the nonwoven mats. Comparisons were made between base mats, CNT-containing mats, and the commercial carbon substrate. In addition, Pt/C sprayed layer uniformity was assessed through SEM scans evaluation.

2.7.2 TEM analysis of local fiber structure and CNT distribution

Transmission electron microscopy (TEM) was used to investigate the local structure of the carbon fibers and the distribution of carbon nanotubes within the lignin-derived mats. TEM images were acquired using a JEOL JEM-2100Plus transmission electron microscope (JEOL Ltd., Japan), operated at 200 kV. TEM analysis provided insights into the internal structure of individual fibers and the interaction between CNTs and the carbon matrix.

2.7.3 BET surface area and pore size distribution (N_2 and CO_2 adsorption–desorption)

Gas adsorption measurements were carried out to characterize the surface area and pore structure of the carbon mats using a Micromeritics TriStar II Plus surface area and porosity analyzer (Micromeritics Instrument Corp., USA). Nitrogen adsorption–desorption isotherms at 77 K were used to determine the specific surface area using the Brunauer–Emmett–Teller (BET) method.
To probe ultramicroporosity that may not be accessible to nitrogen at cryogenic temperature, CO_2 adsorption measurements were performed at 273 K. The Dubinin–Radushkevich (DR) model was applied to the CO_2 adsorption isotherms to estimate the micropore volume and apparent surface area [7].
Pore size distributions were obtained using the non-local density functional theory (NLDFT) model applied to both N_2 (77 K) and CO_2 (273 K) adsorption data.

2.7.4 Raman spectroscopy

Raman spectroscopy was used to assess the structural ordering of the lignin-derived carbon mats. Raman spectra were collected to analyze the characteristic D and G bands of carbon materials. The ID/IG ratio was used as a comparative parameter to evaluate differences in structural order between samples carbonized under different conditions and between lignin-derived mats and the commercial carbon substrate.

2.8 From lignin to spray coated lignin derived mats (LDMs): a summary

The experimental procedure adopted in this work is summarized in Figure 13.

Figure 13 - Schematic overview of the experimental workflow used for the fabrication and testing of lignin-derived electrospun carbon mats.

References

[1] L. Lavagna, M. Bartoli, D. Suarez-Riera, D. Cagliero, S. Musso, and M. Pavese, "Oxidation of Carbon Nanotubes for Improving the Mechanical and Electrical Properties of Oil-Well Cement-Based Composites," *ACS Appl. Nano Mater.*, vol. 5, no. 5, pp. 6671–6678, May 2022, doi: 10.1021/acsanm.2c00706.

[2] M. Zhang, M. Yang, M. Yaguchi, H. Jintoku, S. Sakurai, and D. Futaba, "Understanding and controlling the oxidation degree of single-wall carbon nanotubes: A comparative study of treatment processes," *Carbon N. Y.*, vol. 237, p. 120132, Apr. 2025, doi: 10.1016/j.carbon.2025.120132.

[3] W. C. Teoh, W. M. Yeoh, and A. R. Mohamed, "Evaluation of Different Oxidizing Agents on Effective Covalent Functionalization of Multiwalled Carbon Nanotubes," *Fullerenes Nanotubes and Carbon Nanostructures*, vol. 26, no. 12, pp. 846–850, Dec. 2018, doi: 10.1080/1536383X.2018.1508133.

[4] J. Zhang *et al.*, "Effect of Chemical Oxidation on the Structure of Single-Walled Carbon Nanotubes," *Journal of Physical Chemistry B*, vol. 107, no. 16, pp. 3712–3718, Apr. 2003, doi: 10.1021/jp027500u.

[5] B. C. Kim *et al.*, "Fabrication of enzyme-based coatings on intact multi-walled carbon nanotubes as highly effective electrodes in biofuel cells," *Scientific Reports 2017 7:1*, vol. 7, no. 1, pp. 40202-, Jan. 2017, doi: 10.1038/srep40202.

[6] V. Poursorkhabi, A. K. Mohanty, and M. Misra, "Statistical analysis of the effects of carbonization parameters on the structure of carbonized electrospun organosolv lignin fibers," *J. Appl. Polym. Sci.*, vol. 133, no. 45, Dec. 2016, doi: 10.1002/app.44005.

[7] J. Jagiello, J. Kenvin, A. Celzard, and V. Fierro, "Enhanced resolution of ultra micropore size determination of biochars and activated carbons by dual gas analysis using N2 and CO2 with 2D-NLDFT adsorption models," *Carbon N. Y.*, vol. 144, pp. 206–215, Apr. 2019, doi: 10.1016/j.carbon.2018.12.028.

3 Chapter 3 – Results and Discussion

3.1 Benchmark comparison and contextualization with literature values: lignin-derived electrospun carbon mats vs commercial carbon paper

Before entering the specific structural, textural, surface chemistry and electrochemical analysis of the lignin-derived mats, it is appropriate to start with a comparative assessment against the benchmark material, namely commercial carbon paper. The objective of this comparison is to determine whether lignin can effectively act as a potential substitute for conventional fossil-based substrates, therefore not to highlight superiority, but to verify that the material operates within a range of processability, properties and functionality compatible with the current state of the art.
Carbon paper is commonly used in electrochemical applications due to its well-established electrical conductivity, mechanical robustness, and porous network, which make it versatile and suitable for handling mass transport during different stages of operation [1], [2]. It is therefore necessary to carry out this comparison in order to obtain a clear and realistic framework within which to position the lignin-derived mats, assessing their suitability as free-standing electrode substrates.
The comparison focuses on fiber morphology, including quantitative fiber diameter analysis performed using ImageJ, specific surface area (SSA), pore size distribution (PSD), electrochemical stability in alkaline media and catalytic response under realistic glycerol oxidation conditions.

3.1.1 Morphological comparison of electrode substrates (SEM)

Scanning electron microscopy (SEM) was used to directly compare the morphology of the lignin-derived electrospun carbon mats with that of the commercial carbon paper. Since the morphology of a substrate influences mass transport, catalyst distribution and overall structural behavior, this step is necessary to understand whether the two materials can be realistically compared. As shown in Figure 14.a, the lignin-derived mats show a continuous fibrous network composed of randomly distributed carbon fibers and carbon ribbons. The fibers are in the sub-micrometer range and form an open and interconnected structure. The porosity is clearly visible, with voids distributed throughout the mat thickness.

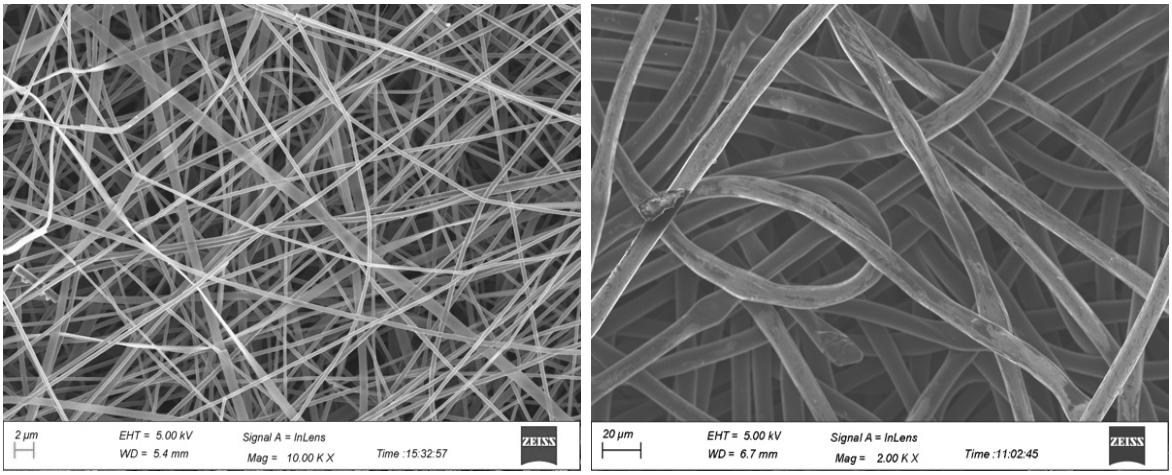

Figure 14 – (a) SEM image of lignin derived carbon mat (b) SEM image of commercial carbon paper Freudenberg H23

The structure reflects the typical nonwoven morphology obtained by electrospinning, where the fibers overlap and create a self-supported network. Image analysis of SEM micrographs performed using ImageJ revealed that the lignin-derived carbon nanofibers exhibit an average diameter of 0.41 ± 0.07 μm, confirming their nanometric nature.
On the other hand, the commercial carbon paper in Figure 14.b presents a more compact and organized fiber structure. The fibers appear thicker and the overall network is denser, which is consistent with its optimized industrial processing and mechanical consolidation. The porosity is still present, but the packing of the fibers is more uniform and controlled.

In contrast, the commercial carbon substrate consists of significantly thicker micrometric fibers with an average diameter of 8.7 ± 1.6 μm, as obtained from the same image analysis procedure. A quantitative analysis of the fiber diameters obtained from SEM micrographs is summarized in Table 4.

Table 4 - Fiber diameter statistics obtained from SEM images using ImageJ.

Sample	Number of fibers (n)	Mean diameter	Standard deviation	Median	Minimum	Maximum
Lignin-derived carbon nanofibers	50	0.41 μm	0.07 μm	0.40 μm	0.29 μm	0.56 μm
Commercial carbon substrate	40	8.7 μm	1.6 μm	8.5 μm	6.1 μm	12.3 μm

Despite these structural differences, both materials exhibit a continuous carbon framework. From a purely morphological point of view, the lignin-derived mats provide an interconnected structure that is compatible with their intended use as free-standing electrode substrates, even if differences in density and fiber packing remain evident.

3.1.2 Textural properties and accessible surface area (BET and PSD)

Nitrogen adsorption measurements were performed to evaluate the specific surface area and accessible porosity of the lignin-derived carbon mats. Since surface area and pore structure influence catalyst dispersion and electrolyte accessibility, this analysis provides an indication of whether the developed materials fall within a functional range compatible with electrochemical electrode substrates. The nitrogen adsorption–desorption isotherm measured at 77 K (Figure 15) confirms the presence of accessible porosity within the carbonized fibrous structure. From the BET analysis, a specific surface area of 281.9 $m^2 g^{-1}$ was obtained. This value reflects the combined contribution of the intrinsic porosity generated during carbonization and the hierarchical void structure of the electrospun non-woven network.

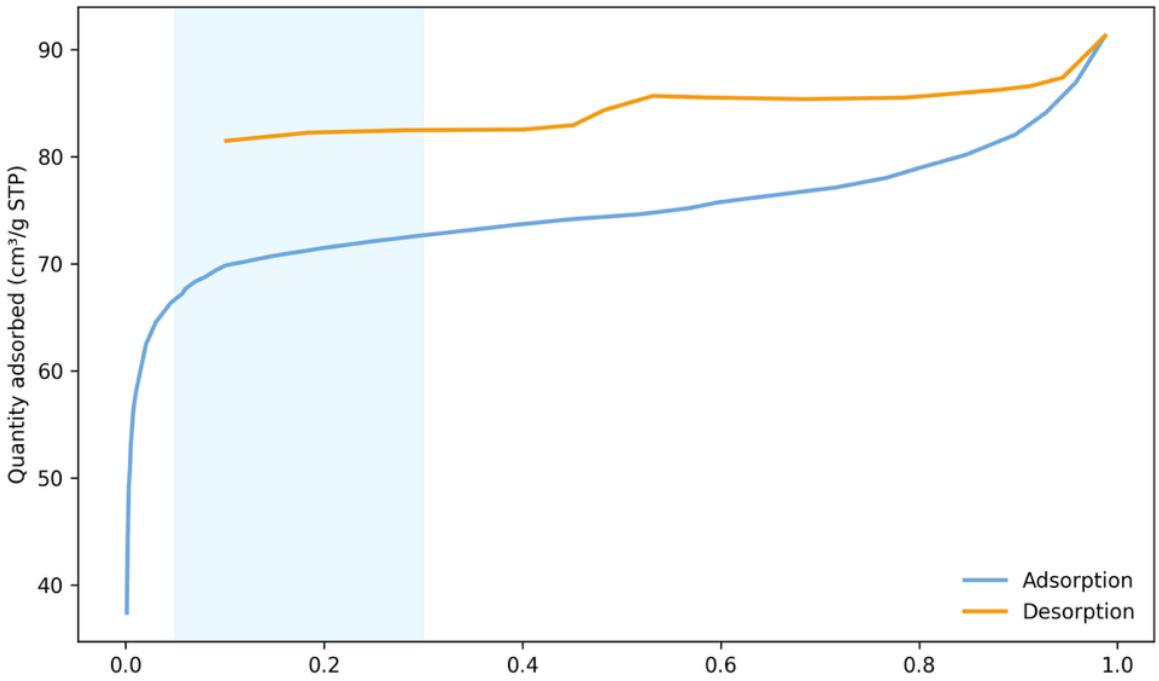

Figure 15 - Nitrogen adsorption–desorption isotherm of the lignin-derived carbon mat measured at 77 K, used to evaluate the specific surface area and accessible porosity of the material.

The pore size distribution derived from N_2 adsorption (Figure 16) indicates a dominant contribution in the microporous region around ~1 nm, together with a smaller fraction of larger pores. However, nitrogen adsorption at 77 K can underestimate the presence of very narrow micropores due to diffusion limitations in ultramicroporous carbon materials.

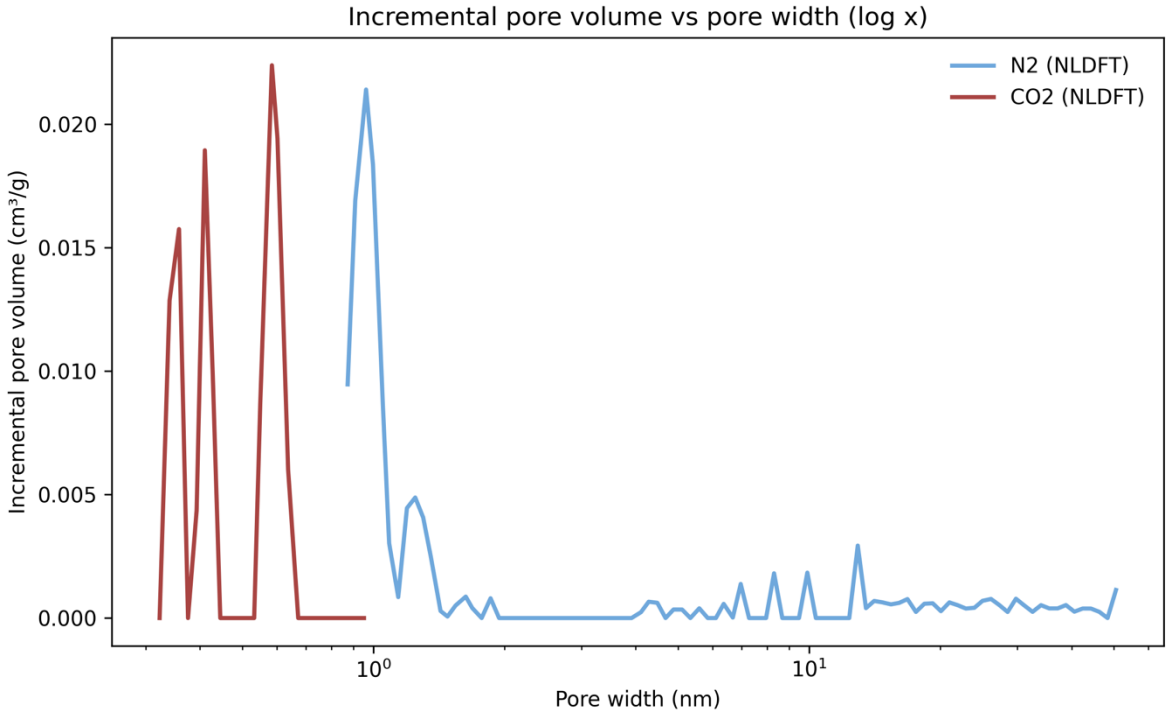

Figure 16 - Combined pore size distribution of the lignin-derived carbon mat derived from N_2 adsorption at 77 K and CO_2 adsorption at 273 K using NLDFT analysis, highlighting the micro- and ultramicroporous regions.

To further investigate this aspect, CO_2 adsorption measurements were performed at 273 K, which are more sensitive to ultramicropores below approximately 0.7 nm. The surface area estimated from CO_2 adsorption using the Dubinin–Radushkevich model resulted in a significantly higher value of 517.2 $m^2\ g^{-1}$, indicating the presence of a substantial ultramicroporous fraction not fully accessible to nitrogen.
The combined pore size distribution obtained from N_2 and CO_2 adsorption (Figure 16) confirms that the porosity of the lignin-derived carbon mats is mainly located in the micro- and ultramicroporous range, which likely originates from structural rearrangements of the lignin-based carbon matrix during thermal treatment rather than from chemical activation processes. Although microporosity does not directly enhance macroscopic mass transport, it increases the available surface for catalyst anchoring and interfacial interactions. At the same time, the fibrous architecture of the electrospun mats provides larger inter-fiber voids, which facilitate electrolyte penetration and mass transport at the structural scale.
A direct BET measurement of the commercial carbon paper used as benchmark (Freudenberg H23) was not performed in this work. However, literature reports indicate that conventional carbon papers typically exhibit relatively low intrinsic surface areas, ranging approximately from 1 to 53 $m^2\ g^{-1}$, depending on thermal treatment conditions [3]. These materials rely primarily on their conductive carbon network and structural robustness rather than on high internal surface area. An overall summary of obtained and reported SSA's is shown in Table 5.

Table 5 - Comparison of the specific surface area (SSA) of the lignin-derived carbon mat obtained from N_2 adsorption at 77 K (BET method) and CO_2 adsorption at 273 K (Dubinin–Radushkevich method) with literature range of values reported for commercial carbon paper (Freudenberg H23) which depend on thermal treatment [3].

SSA Freudenberg H23	SSA LDM N_2@77K BET	SSA LDM CO_2@273K Dubinin-Radushkevich
~1-53.6 m^2/g	281.9 m^2/g	517.2 m^2/g

Within this framework, the surface area and pore structure measured for the lignin-derived mats place them in an intermediate regime where significant accessible surface is achieved without aggressive activation, while maintaining the structural integrity required for free-standing electrode substrates.
Indeed, a high specific surface area is not necessarily the primary requirement for electrochemical substrate materials. In many practical electrode architectures, an optimal balance between accessible surface area, pore structure, electrical conductivity and structural integrity is more critical than maximizing porosity alone. Excessive microporosity can increase surface area but may also limit effective mass transport and compromise mechanical robustness, particularly in free-standing fibrous substrates. In this context, the lignin-derived carbon mats developed in this work fall within a functional regime where moderate surface area is combined with a continuous conductive carbon network and an open fibrous architecture, which together support efficient electrolyte penetration and electron transport during electrochemical operation. Similar considerations have been reported for commercial carbon papers used as electrode substrates, where performance is governed by the interplay between conductivity, pore architecture and structural stability rather than by surface area alone [4], [5].

3.1.3 Electrochemical response in alkaline electrolyte (CV in 1 M NaOH)

The electrochemical response of the lignin-derived carbon mats was first evaluated in a blank alkaline electrolyte in order to assess their intrinsic electrochemical behavior prior to glycerol oxidation. Cyclic voltammetry measurements were therefore performed in 1 M NaOH using a three-electrode configuration. The potentials were measured against a Hg/HgO reference electrode and subsequently converted to the reversible hydrogen electrode (RHE) scale to facilitate comparison with literature data.
Figure 17 shows the cyclic voltammograms recorded for the lignin-derived mat (LDM) and for the commercial carbon paper benchmark (Freudenberg H23) in NaOH 1M solution.

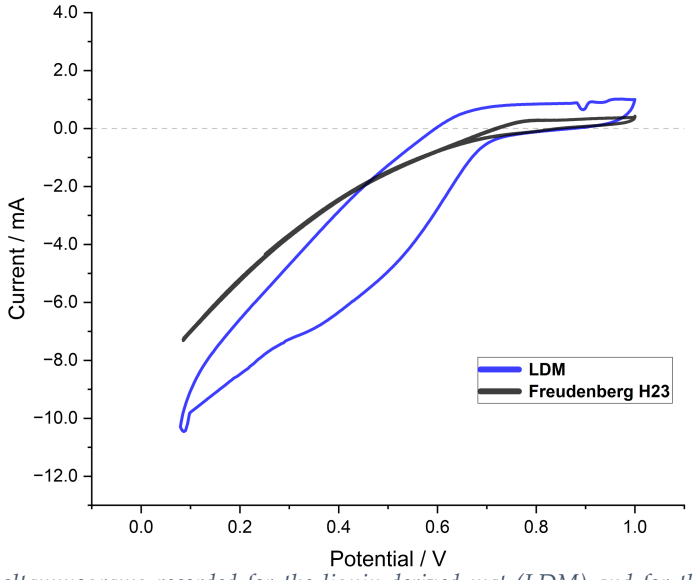

Figure 17 - Cyclic voltammograms recorded for the lignin-derived mat (LDM) and for the commercial carbon paper benchmark Freudenberg H23 in NaOH 1M solution. The potential has been converted to RHE for clearer comparison with literature. Only the last 2 cycles of the 50 total cycles have been reported.

Both materials exhibit a similar electrochemical potential window in the investigated range, indicating that the lignin-derived carbon substrate remains electrochemically stable under alkaline conditions.
A noticeable difference between the two electrodes is the higher background current observed for the LDM sample. This behavior is attributed to an increased capacitive contribution, which likely originates from the larger accessible surface area and the presence of micro- and ultramicroporosity previously identified through gas adsorption measurements. The larger interfacial area between the carbon surface and the electrolyte results in a higher electrochemical double-layer capacitance, which manifests as an increased capacitive current during the potential sweep [2], [4].
Despite this difference in capacitive response, both materials show stable and reproducible voltammetric profiles without signs of significant degradation within the investigated potential range. This confirms that the lignin-derived carbon mats possess good electrochemical stability in alkaline media, making them suitable candidates as electrode substrates for subsequent catalytic experiments.
Overall, the electrochemical response observed in alkaline electrolyte is consistent with the structural characteristics identified through gas adsorption analysis, where the combination of intrinsic microporosity and the open fibrous architecture contributes to an increased electrochemically accessible surface.

3.1.4 Electrocatalytic performance in glycerol electrooxidation (1 M NaOH + 1 M glycerol)

The electrocatalytic performance of the lignin-derived carbon mats was evaluated through cyclic voltammetry in the presence of glycerol in order to assess their suitability as electrode substrates for biomass electro-oxidation reactions. The measurements were carried out in an electrolyte containing 1 M NaOH and 1 M glycerol using the same three-electrode configuration described previously. The potentials were measured against a Hg/HgO reference electrode. Figure 18 shows the cyclic voltammograms recorded for the lignin-derived mat (LDM) and for the commercial carbon paper benchmark (Freudenberg H23) under identical experimental conditions. In both cases, the catalyst loading was maintained constant at 0.19 mgPt cm^{-2} to ensure a meaningful comparison between the two electrode substrates.

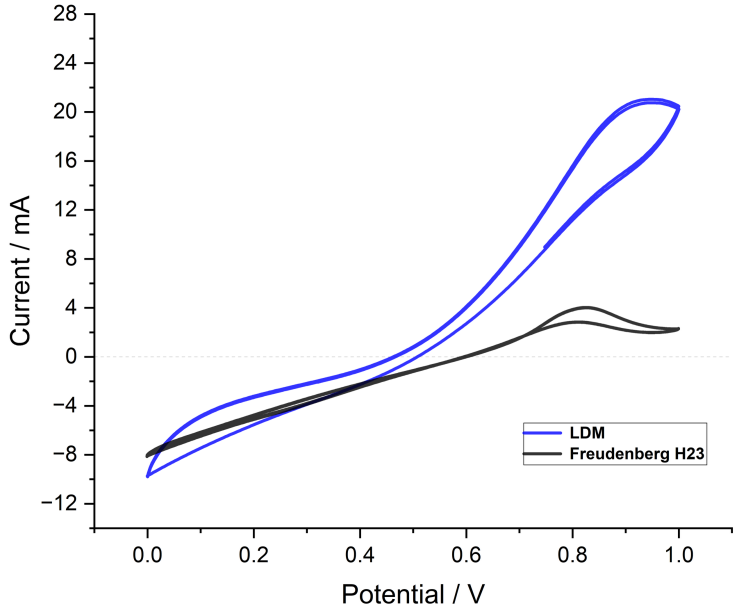

Figure 18 - Cyclic voltammograms recorded for the lignin-derived mat (LDM) and for the commercial carbon paper benchmark Freudenberg H23 in glycerol 1 M and NaOH 1 M solution. The potential has been converted to RHE for clearer comparison with literature. Only the last 2 cycles of the 50 total cycles have been reported.

In the presence of glycerol, a clear increase in anodic current is observed at higher potentials, corresponding to the onset of the glycerol electrooxidation reaction (GOR).

While both electrodes display catalytic activity toward glycerol oxidation, the lignin-derived mat exhibits significantly higher oxidative currents across the investigated potential range compared to the commercial carbon paper.
This difference can be partially attributed to the higher capacitive background observed for the LDM electrode, which reflects a larger electrochemically accessible surface area. As previously discussed in the gas adsorption analysis and the blank electrolyte voltammetry, the lignin-derived carbon mats possess a more developed micro- and ultramicroporous structure. This increased interfacial area likely promotes improved catalyst dispersion and enhanced interaction between the catalyst layer and the electrolyte.
Additionally, the fibrous architecture of the electrospun mats may contribute to improved accessibility of the catalytic sites by facilitating electrolyte penetration and providing a highly open conductive network. These structural features can enhance the effective utilization of the deposited platinum catalyst during the electrooxidation reaction.
Although a detailed kinetic analysis is beyond the scope of this preliminary comparison, the results indicate that the lignin-derived carbon mats can support catalytic activity for glycerol electrooxidation at levels comparable or superior to the commercial carbon substrate used as benchmark. This observation further supports the potential of lignin-derived electrospun carbon materials as sustainable alternatives to conventional fossil-derived electrode substrates.
Further investigations will be required to decouple the contributions of capacitive currents and intrinsic catalytic activity.

3.2 Effect of fiber morphology and carbonization temperature

The carbonization temperature plays a critical role in determining the structural properties of lignin-derived carbon materials, influencing both the morphology of the fibrous network and the degree of structural ordering of the resulting carbon matrix. For this reason, lignin-derived electrospun mats were carbonized at three different temperatures, namely 800 °C, 1000 °C and 1200 °C, in order to evaluate how the thermal treatment affects the morphology and graphitic character of the fibers.
The resulting materials were characterized through scanning electron microscopy (SEM) to investigate potential morphological changes in the fibrous network, and Raman spectroscopy to assess the evolution of structural ordering in the carbon matrix. These complementary techniques allow correlating macroscopic morphology with the microscopic ordering of carbon domains.
Understanding these effects is essential for identifying a suitable carbonization temperature that balances structural integrity, electrical properties and process stability, which are all critical parameters for electrode substrate applications.

3.2.1 SEM analysis of lignin-derived mats carbonized at different temperatures

Scanning electron microscopy images of the lignin-derived mats carbonized at 800 °C, 1000 °C and 1200 °C are shown in Figure 19.

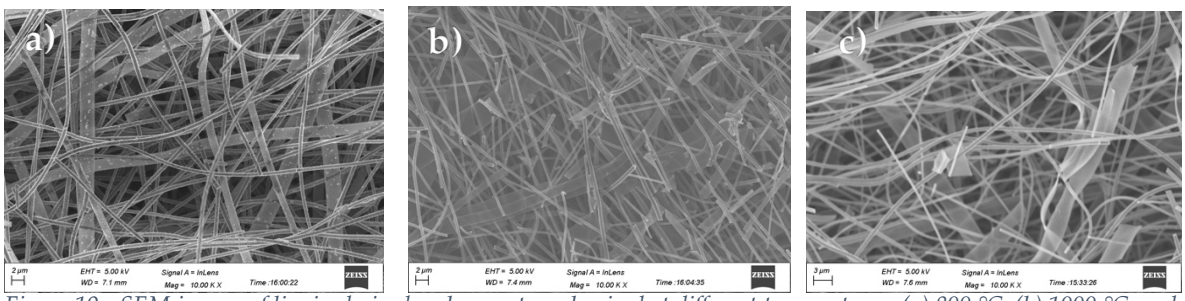

Figure 19 - SEM images of lignin-derived carbon mats carbonized at different temperatures: (a) 800 °C, (b) 1000 °C, and (c) 1200 °C.

Overall, the fibrous morphology produced during the electrospinning step is largely preserved after carbonization across the entire temperature range investigated. The SEM images reveal a continuous non-woven network of randomly oriented fibers, with no

evidence of extensive fiber fusion or collapse during thermal treatment. This observation suggests that the carbonization process proceeds without significant melting or restructuring of the fiber network.
The preservation of the fibrous architecture indicates that the lignin-based precursor undergoes carbonization while maintaining the original electrospun structure. This behavior is consistent with the thermally induced decomposition of the polymeric components and the formation of a carbonaceous framework during pyrolysis.
No major morphological differences are observed between samples carbonized at 800 °C and 1000 °C, where the fibrous network remains homogeneous and well preserved. In contrast, the material carbonized at 1200 °C appears slightly more fragile during handling, suggesting that excessively high temperatures may lead to a more brittle carbon structure.
Overall, the SEM observations confirm that the electrospun architecture is maintained throughout carbonization, ensuring the formation of a highly open fibrous structure that is favorable for electrolyte penetration and catalyst deposition in electrochemical applications.

3.2.2 Raman spectroscopy: structural ordering and ID/IG evolution

Raman spectroscopy was used to evaluate the structural ordering of the carbon matrix as a function of carbonization temperature. The Raman spectra of the samples carbonized at 800 °C, 1000 °C and 1200 °C are presented in Figure 20. While SEM images did not show visible morphological differences between 800 °C, 1000 °C and 1200 °C, Raman allows us to observe structural changes occurring at the molecular level.

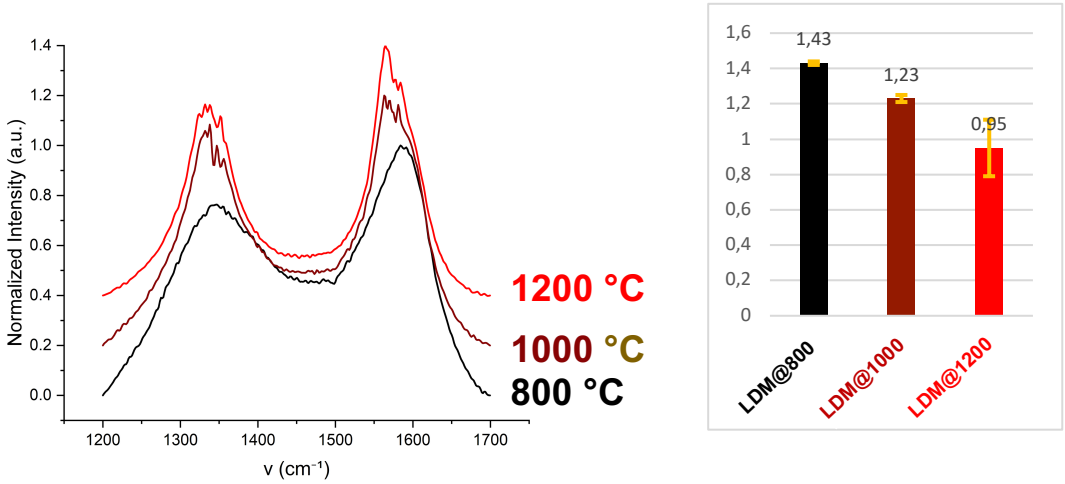

Figure 20 – Raman spectra of LDM@800, LDM@1000 and LDM@1200, normalized and vertically shifted for clarity and corresponding bar chart of ID/IG ratio with mean ± SD of LDMs carbonized at different temperatures. Peak deconvolution of the D and G bands was performed using pseudo-Voigt functions.

All spectra display the characteristic D band (~1350 cm^{-1}) and G band (~1580 cm^{-1}) typical of disordered carbon materials. The D band is associated with structural defects and disorder in the carbon lattice, while the G band corresponds to the in-plane vibration of sp^2-bonded carbon atoms in graphitic structures.
A progressive change in the ID/IG ratio is observed as the carbonization temperature increases. The sample carbonized at 800 °C exhibits the highest ID/IG value (~1.43), indicating a relatively high degree of structural disorder. Increasing the temperature to 1000 °C results in a decrease of the ID/IG ratio (~1.23), suggesting the development of a more ordered carbon structure. A further reduction is observed for the material carbonized at 1200 °C, where the ID/IG ratio decreases to approximately 0.95, indicating a higher degree of graphitic ordering.
This trend is consistent with the progressive aromatization and structural rearrangement of the carbon matrix occurring at higher temperatures during pyrolysis.
However, considering both structural ordering and practical handling properties, the sample carbonized at 1000 °C was selected as the reference material for subsequent

experiments. While the material carbonized at 1200 °C exhibits a slightly higher degree of structural ordering, it was found to be more brittle during handling. On the other hand, carbonization at 800 °C may leave a larger fraction of residual oxygen-containing functionalities within the carbon structure.
Therefore, 1000 °C represents a suitable compromise, providing sufficient carbon ordering while maintaining adequate mechanical integrity of the fibrous mat.

3.3 Incorporation of carbon nanotubes: structural and functional implications

While the lignin-derived carbon mats exhibited promising electrochemical behavior and higher oxidative currents compared to the commercial carbon paper benchmark, an important limitation was observed during practical handling of the materials. The carbonized mats were found to be relatively brittle and mechanically fragile, which may limit their robustness as free-standing electrode substrates.
This behavior is commonly observed in lignin-derived carbon materials, where the carbonization of biopolymer precursors can lead to rigid and brittle carbon frameworks.
To address this limitation, the incorporation of carbon nanotubes (CNTs) was explored as a potential strategy to reinforce the fibrous structure. Due to their high electrical conductivity, mechanical strength, and high aspect ratio, CNTs can act both as conductive bridges between carbon fibers and as structural reinforcement within the carbon matrix.
Therefore, CNTs were introduced into the electrospinning formulation in order to improve the mechanical robustness and electrical connectivity of the lignin-derived carbon mats while maintaining the advantageous porous fibrous architecture.

3.3.1 Morphology of CNTs loaded lignin-derived mats (SEM) and final nanocomposite concentrations

To investigate the effect of carbon nanotube incorporation on the structure of the electrospun mats, CNTs were introduced into the electrospinning formulation at different loadings. Two concentrations were explored, corresponding to 0.5 wt% and 0.75 wt% relative to the total solid content of the spinning solution, resulting in the samples hereafter referred to as LDM0.5CNT and LDM0.75CNT, respectively.
Scanning electron microscopy images of the resulting carbonized mats are presented in Figure 21, together with the reference lignin-derived mat without CNTs.

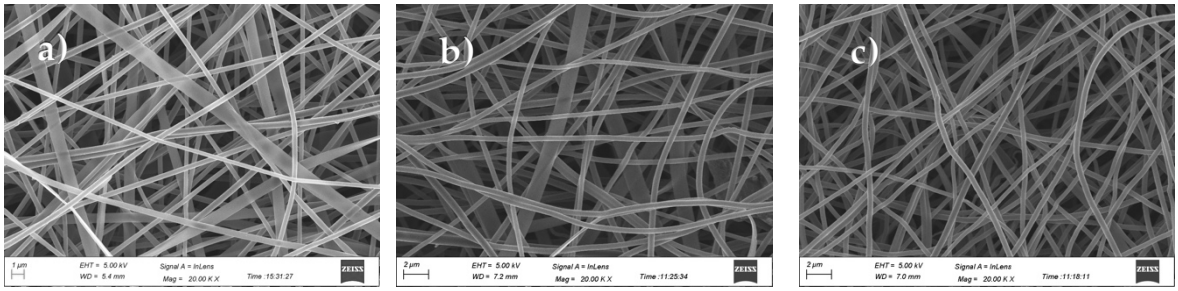

Figure 21 - SEM images of carbonized lignin-derived mats: (a) LDM (reference sample without CNTs), (b) LDM0.5CNT and (c) LDM0.75CNT.

In all cases, the electrospun structure is preserved after carbonization, showing a randomly oriented fibrous network typical of electrospun carbon mats.
The incorporation of CNTs at the investigated concentrations does not lead to significant alterations of the overall fibrous morphology. The fibers remain continuous and well distributed within the non-woven network, and no clear evidence of fiber fusion or structural collapse is observed. The general architecture of the electrospun mat therefore remains largely unchanged upon CNT addition.
At the scale accessible through SEM imaging, the presence of CNTs is not clearly distinguishable within the fibers or at the fiber surface. This behavior is expected given the

apparently low CNT loading used in the formulation and their nanoscale dimensions compared to the micrometer-scale diameter of the electrospun fibers.
It is important to note that the final CNT concentration in the carbonized mats is higher than the initial loading in the spinning formulation. This is due to the mass loss associated with lignin carbonization during pyrolysis, alongside PEO that completely undergoes pyrolisis. Assuming a carbon yield of approximately 30 wt% for organosolv lignin, the CNT fraction in the final carbon materials increases to approximately 1.4 wt% for LDM0.5CNT and 2.2 wt% for LDM0.75CNT, as summarized in previously mentioned Table 3. These values provide an estimate of the effective CNT content in the final carbon nanocomposite, which is consistent with nano-reinforcement content for nanocomposites in literature.

3.3.2 Raman spectroscopy of CNT-reinforced mats

To further investigate the effect of CNT incorporation on the carbon structure of the electrospun mats, Raman spectroscopy was performed on the CNT-reinforced samples and compared with the reference lignin-derived carbon mat.
The Raman spectra of LDM, LDM0.5CNT and LDM0.75CNT are shown in Figure 22.

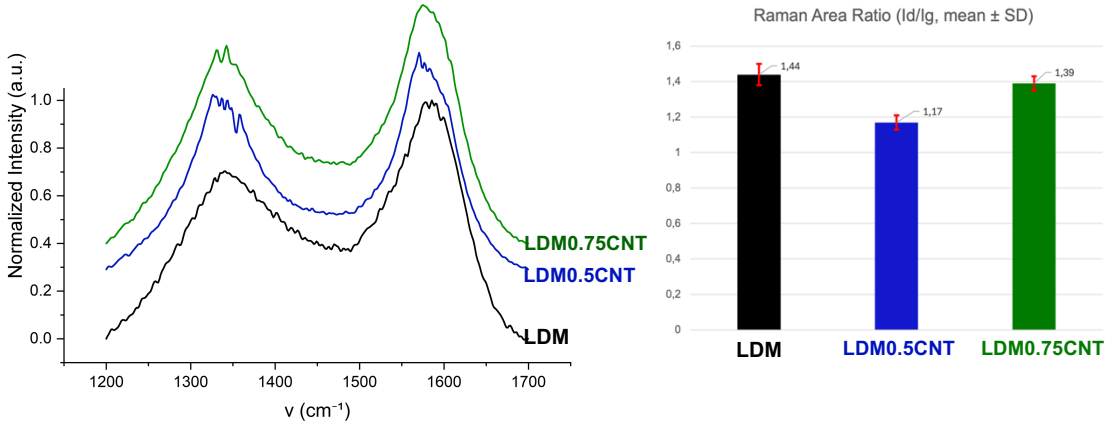

Figure 22 - Raman spectra of LDM, LDM0.5CNT and LDM0.75CNT and corresponding ID/IG ratios highlighting the increase in structural disorder at higher CNT loading. Peak deconvolution of the D and G bands was performed using pseudo-Voigt functions.

All samples display the characteristic D band (~1350 cm^{-1}) and G band (~1580 cm^{-1}) typical of disordered carbon materials. However, noticeable differences are observed in the ID/IG ratio, which reflects the degree of structural disorder within the carbon matrix.
As summarized in Figure 22, the sample containing 0.5 wt% CNT exhibits a slightly lower ID/IG ratio compared to the reference LDM, suggesting that small additions of CNTs may contribute to improving local structural ordering or electrical connectivity within the carbon network. In contrast, the sample containing 0.75 wt% CNT shows an increase in the ID/IG ratio, indicating a higher degree of structural disorder.
This behavior suggests that higher CNT concentrations may lead to local structural heterogeneities within the electrospun fibers. One possible explanation is the formation of CNT aggregates within the precursor solution, which could interfere with the formation of a homogeneous lignin-based carbon matrix during electrospinning and subsequent carbonization [6]. It should also be noted that carbon nanotubes possess a strong tendency to form bundles due to van der Waals interactions between adjacent tubes. This intrinsic aggregation behavior can limit their dispersion within polymeric precursor solutions and may explain the formation of localized CNT clusters observed in the TEM images at higher loadings.
Based on this observation, a schematic representation of the possible CNT distribution within the fibers is proposed in Figure 23, where at lower CNT loadings the nanotubes are relatively well dispersed within the lignin matrix, while at higher concentrations they may form localized clusters or aggregates.

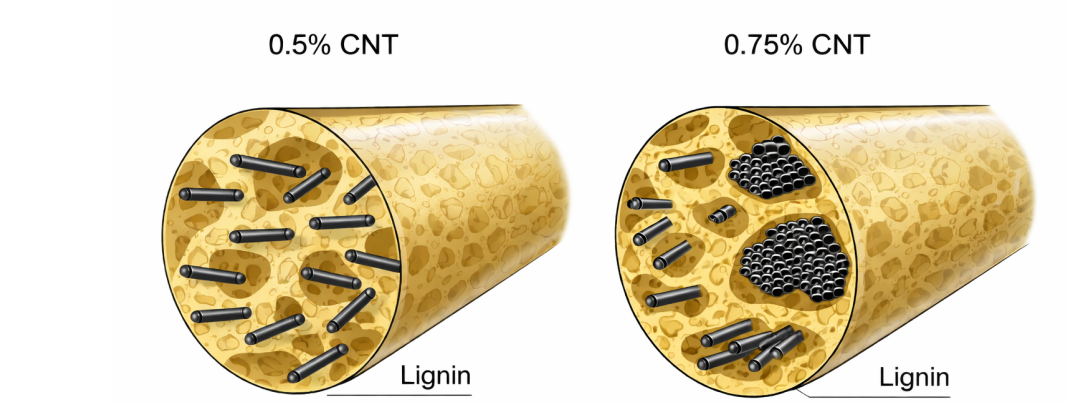

Figure 23 – Schematic of hypothetical CNT distribution in samples LDM0.5CNT and LDM0.75CNT. Illustration by author.

To further explore this hypothesis, transmission electron microscopy (TEM) was used to examine the nanoscale structure of the CNT-containing mats. Representative TEM images are shown in Figure 24.

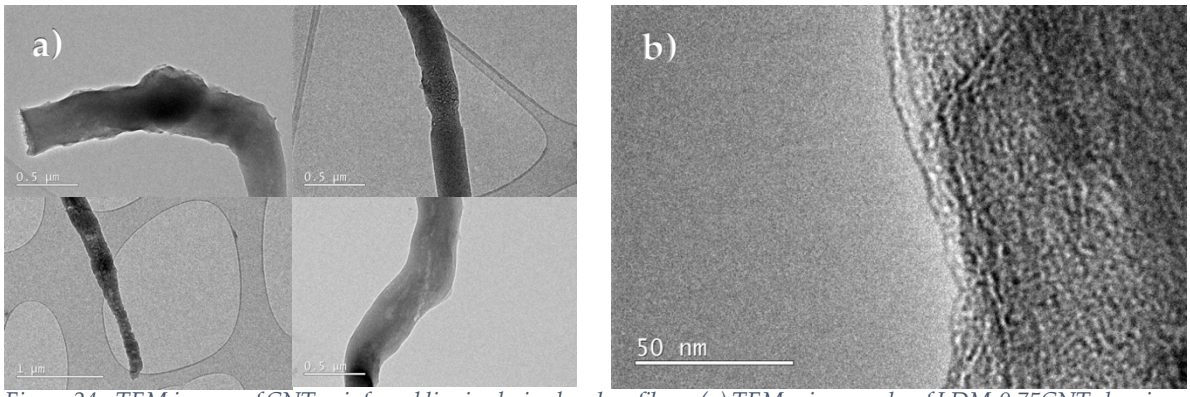

Figure 24 - TEM images of CNT-reinforced lignin-derived carbon fibers. (a) TEM micrographs of LDM-0.75CNT showing structural defects and dense dark "blob-like" domains, attributed to local aggregates of carbon nanotubes embedded within the carbonized fiber. (b) Higher-magnification TEM image of LDM-0.5CNT suggesting the presence of an individual carbon nanotube located at the fiber surface.

At higher CNT loading, several regions appear as dense dark domains or "blob-like" structures, which are consistent with CNT aggregates embedded within the carbonized fibers. These features can locally disrupt the formation of a uniform carbon matrix and may explain the increase in structural disorder observed in the Raman analysis.
In contrast, such aggregated structures are less evident in the material containing 0.5 wt% CNT, suggesting a more homogeneous dispersion at lower nanotube concentrations.
Additionally, high-magnification TEM images reveal elongated nanostructures located at or near the surface of the carbon fibers, which are consistent with individual carbon nanotubes positioned along the fiber surface. These observations support the idea that CNTs can act as conductive bridges within the fibrous network, while excessive concentrations may lead to aggregation phenomena.
Overall, the combined Raman and TEM analyses suggest that moderate CNT incorporation may be beneficial for the structural organization of the carbon mats, whereas higher CNT loadings may lead to aggregation and increased structural disorder within the fibers.

3.4 Overall assessment of lignin-derived carbon mats as electrode substrates

After evaluating the morphology, textural properties and structural characteristics of the developed materials, it is necessary to assess their overall electrochemical performance as electrode substrates. In particular, the comparison between lignin-derived mats and commercial carbon paper provides an indication of whether these bio-based materials can realistically operate within the functional range required for electrochemical applications.
In addition to the reference lignin-derived mat (LDM), the CNT-reinforced samples (LDM0.5CNT and LDM0.75CNT) were also considered in order to understand whether the incorporation of conductive nanostructures could improve the electrochemical response of the system. The comparison therefore focuses on the electrochemical behavior of the different materials in alkaline electrolyte and during glycerol electro-oxidation.
This analysis makes it possible to identify both the advantages and the current limitations of lignin-derived electrospun carbon mats, and to discuss their potential implications for the design of sustainable carbon electrode substrates.

3.4.1 Electrochemical comparison of the developed electrodes

To further assess the electrochemical behavior of the developed materials, cyclic voltammetry measurements were performed both in alkaline electrolyte (1 M NaOH) and in the presence of glycerol (1 M NaOH + 1 M glycerol). These measurements allow a direct comparison between the commercial carbon paper (Freudenberg H23), the pristine lignin-derived mats (LDM), and the CNT-reinforced samples.
First, the baseline electrochemical response of the materials was evaluated in 1 M NaOH (Figure 25).

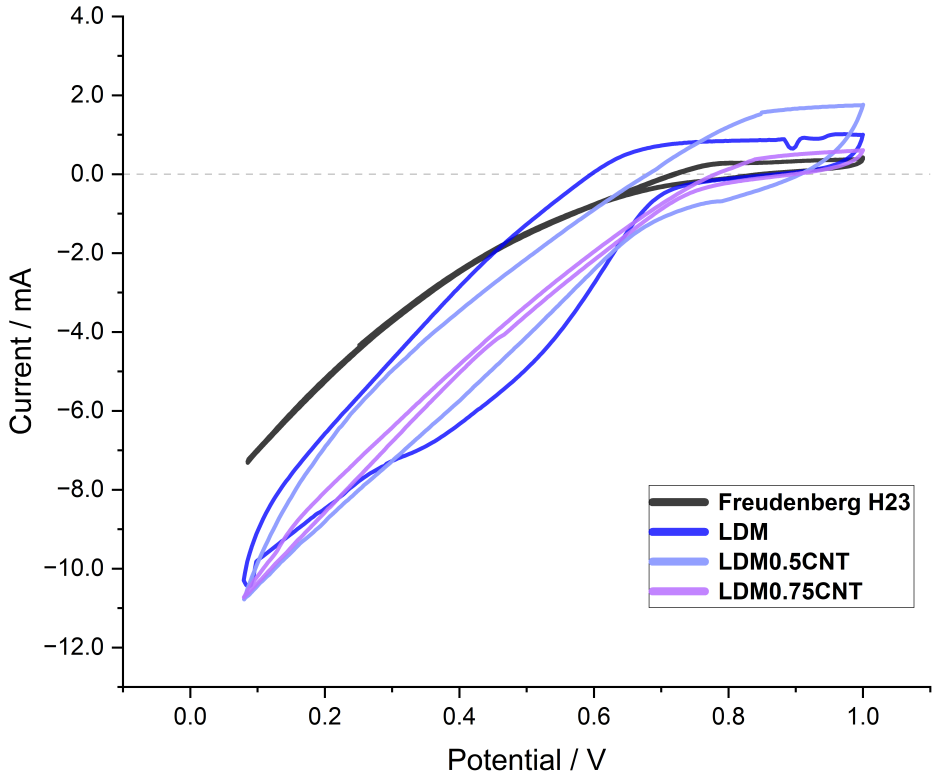

Figure 25 - Cyclic voltammograms recorded for all the lignin-derived mats (LDMs) and for the commercial carbon paper benchmark Freudenberg H23 in NaOH 1M solution. The potential has been converted to RHE for clearer comparison with literature. Only the last 2 cycles of the 50 total cycles have been reported.

The cyclic voltammograms show that all samples operate within a comparable electrochemical window, indicating that the incorporation of carbon nanotubes does not introduce evident instability or parasitic reactions in alkaline medium.

The pristine LDM exhibits a higher capacitive current compared to the commercial carbon paper, which can be attributed to its higher accessible surface area and porous fibrous structure. The CNT-reinforced samples display a similar overall behavior, confirming that the incorporation of nanotubes does not significantly alter the baseline electrochemical stability of the material.
A slightly reduced capacitive response is observed for the sample containing the higher CNT loading (LDM0.75CNT). However, since only a limited number of measurements were performed due to time constraints, further repetitions would be necessary to determine whether this difference reflects an intrinsic property of the material or simply experimental variability.
The electrocatalytic response of the materials was then evaluated in the presence of glycerol (Figure 26).

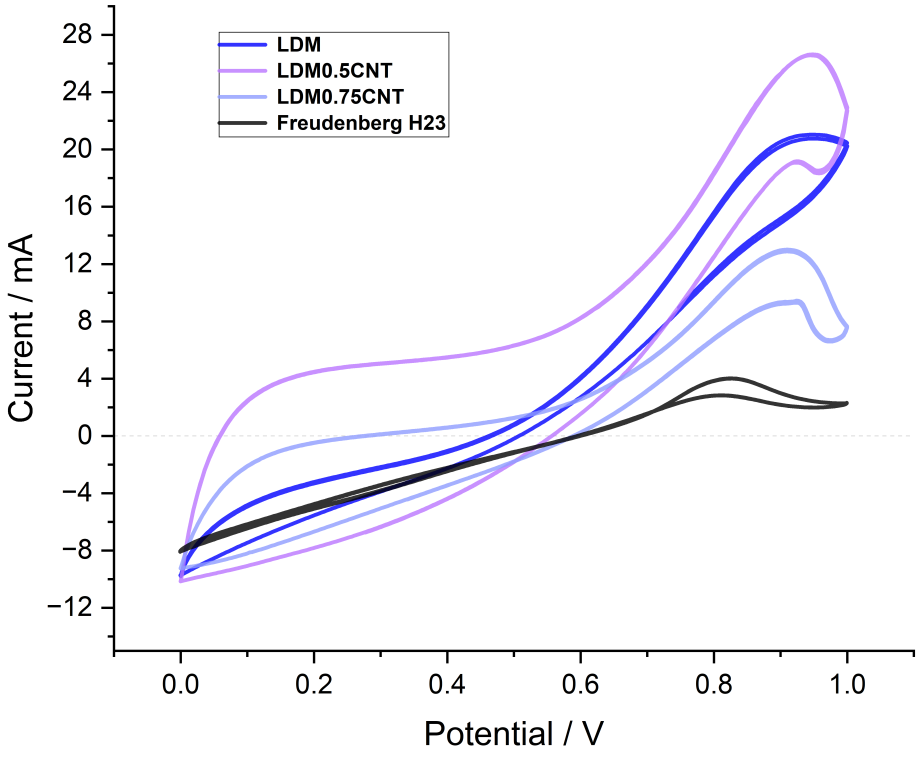

Figure 26 - Cyclic voltammograms recorded for all the lignin-derived mats (LDMs) and for the commercial carbon paper benchmark Freudenberg H23 in glycerol 1 M and NaOH 1 M solution. The potential has been converted to RHE for clearer comparison with literature. Only the last 2 cycles of the 50 total cycles have been reported.

In this case, clear differences between the samples emerge. Compared to both the pristine LDM and the commercial carbon paper, the sample containing the lower CNT loading (LDM0.5CNT) exhibits an increase in oxidative current, suggesting a more favorable electrochemical response for glycerol electrooxidation.
Interestingly, the sample containing the higher CNT concentration (LDM0.75CNT) shows a reduction in performance relative to LDM0.5CNT. This behavior is consistent with the structural observations discussed in the previous section, where TEM images suggested the formation of CNT aggregates at higher loadings. Such aggregates may locally disrupt the fiber structure and reduce the electron transport efficiency and effective accessibility of catalytic sites, thereby limiting the overall electrochemical performance.
Overall, these results suggest that a moderate incorporation of carbon nanotubes can enhance the electrochemical response of lignin-derived carbon mats, while excessive CNT loading may negatively affect performance due to structural heterogeneities and aggregation phenomena.

3.4.2 Advantages, limitations, and implications for substrate design

The results obtained in this work highlight both the potential and the current limitations of lignin-derived electrospun carbon mats as electrode substrates for electrochemical applications.

One of the main advantages of the developed materials lies in their intrinsically porous fibrous structure. The electrospinning process generates a nonwoven network of interconnected carbon fibers, which provides both structural macroporosity and accessible surface area. This architecture facilitates electrolyte penetration and allows the catalyst layer to interact with a relatively large electrochemically active surface. In addition, the use of lignin as a precursor represents a sustainable alternative to conventional fossil-derived carbon materials.

The electrochemical measurements indicate that these lignin-derived mats operate within a stable potential window in alkaline electrolyte and can support glycerol electrooxidation when loaded with platinum catalyst. Compared to the commercial carbon paper used as benchmark, the materials developed in this work exhibit comparable electrochemical behavior and, in some cases, higher oxidative currents during glycerol electrooxidation.

The incorporation of carbon nanotubes was explored as a strategy to improve the mechanical and conductive properties of the mats. At moderate loading (LDM0.5CNT), the presence of CNTs appears to enhance the electrochemical response, likely due to improved electronic pathways and increased local conductivity within the fibrous network.

However, several limitations were also observed. First, the carbonized lignin mats exhibit relatively low mechanical robustness, resulting in brittle structures that may complicate handling and integration into electrochemical devices. Second, increasing the CNT loading beyond a certain threshold leads to aggregation phenomena, as suggested by TEM observations. These aggregates may locally disrupt the fiber formation during electrospinning and reduce the effective accessibility of active sites, ultimately limiting electrochemical performance.

Taken together, these results suggest that lignin-derived electrospun carbon mats represent a promising platform for the development of sustainable electrode substrates. Nevertheless, further optimization of fiber density, CNT dispersion and mechanical stability will be necessary in order to fully exploit their potential in practical electrochemical systems.

3.5 Brief surface characterization before and after catalysis (SEM)

Surface morphology of the lignin-derived mats was examined before and after electrochemical testing using scanning electron microscopy (Figure 27). The SEM images acquired prior to catalysis confirm the preservation of the interconnected fibrous network typical of the platinum on carbon spray coated electrospun structure.

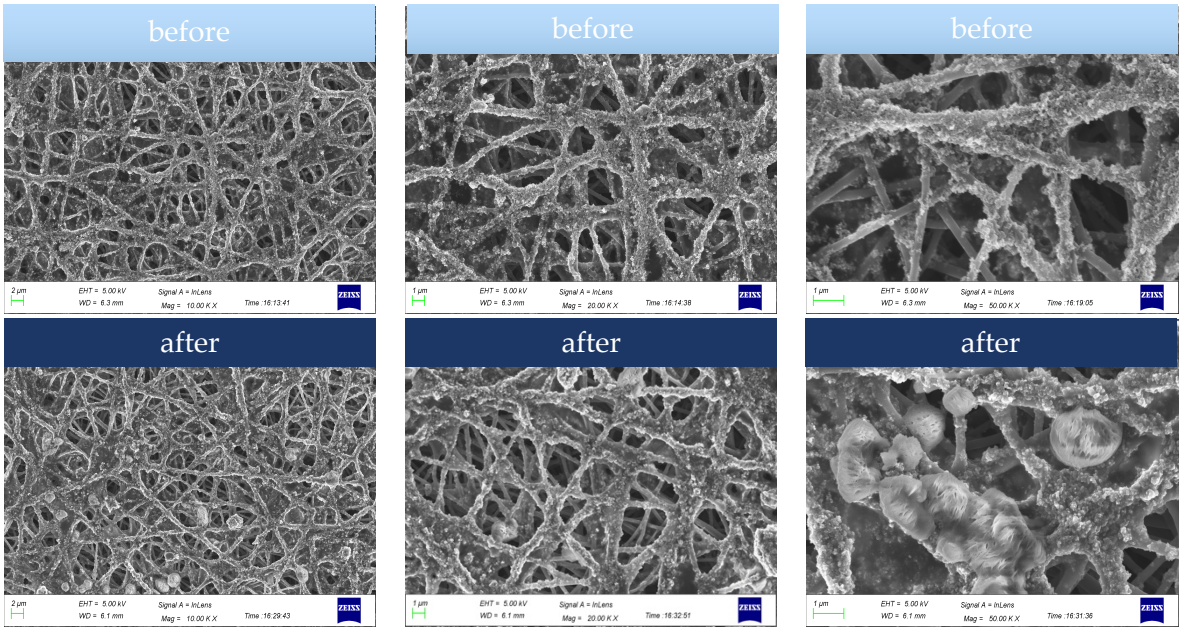

Figure 27 - SEM images of lignin-derived carbon mats before (top row) and after (bottom row) electrochemical glycerol oxidation at increasing magnifications. The images highlight the morphology of the spray coated fibrous carbon network and its evolution after electrochemical operation. Scale bars increase from left to right.

After electrochemical operation in glycerol-containing alkaline electrolyte, noticeable changes in the surface morphology can be observed. In particular, the post-catalysis images reveal the presence of irregular surface deposits distributed along the carbon fibers. These features appear as nodular or clustered structures that were not present in the pristine samples.

Such structures are likely associated with the accumulation of reaction intermediates or oxidation products formed during the glycerol electrooxidation reaction. The electrochemical oxidation of glycerol on Pt-based catalysts is known to generate a wide range of partially oxidized compounds, including glyceraldehyde, dihydroxyacetone and glycerate species, which can adsorb on the catalyst surface during operation [7]. In alkaline media, these intermediates may remain temporarily bound to the catalytic sites or undergo further transformations, potentially leading to the formation of surface deposits.

Although SEM analysis alone cannot determine the precise chemical composition of these structures, their presence suggests the formation of reaction-derived surface species during electrochemical operation. Importantly, the overall fibrous architecture of the carbon mat remains largely preserved, indicating that the substrate maintains its structural integrity under the applied electrochemical conditions.

Further chemical characterization (e.g., XPS or EDX mapping) would be required to identify the exact nature of these surface species.

References

[1] E. Svinterikos, I. Zuburtikudis, and M. Al-Marzouqi, "Electrospun Lignin-Derived Carbon Micro- And Nanofibers: A Review on Precursors, Properties, and Applications," Sep. 21, 2020, *American Chemical Society*. doi: 10.1021/acssuschemeng.0c03246.

[2] F. J. García-Mateos, R. Ruiz-Rosas, J. M. Rosas, J. Rodríguez-Mirasol, and T. Cordero, "Controlling the composition, morphology, porosity, and surface chemistry of

lignin-based electrospun carbon materials," Apr. 15, 2019, *Frontiers Media S.A.* doi: 10.3389/fmats.2019.00114.

[3] K. V. Greco, J. K. Bonesteel, N. Chanut, C. Tai-Chieh Wan, Y. M. Chiang, and F. R. Brushett, "Limited Accessibility to Surface Area Generated by Thermal Pretreatment of Electrodes Reduces Its Impact on Redox Flow Battery Performance," *ACS Appl. Energy Mater.*, vol. 4, no. 12, pp. 13516–13527, Dec. 2021, doi: 10.1021/acsaem.1c01980.

[4] X. Wu *et al.*, "Lignin-derived electrochemical energy materials and systems," May 01, 2020, *John Wiley and Sons Ltd*. doi: 10.1002/bbb.2083.

[5] T. Wang, Z. Liu, P. Li, H. Wei, K. Wei, and X. Chen, "Lignin-derived carbon aerogels with high surface area for supercapacitor applications," *Chemical Engineering Journal*, vol. 466, Jun. 2023, doi: 10.1016/j.cej.2023.143118.

[6] L. M. Ericson and P. E. Pehrsson, "Aggregation Effects on the Raman Spectroscopy of Dielectrophoretically Deposited Single-Walled Carbon Nanotubes," 2005, doi: 10.1021/jp052364p.

[7] Y. Liu, W. Yu, D. Raciti, D. H. Gracias, and C. Wang, "Electrocatalytic Oxidation of Glycerol on Platinum," *The Journal of Physical Chemistry C*, vol. 123, no. 1, pp. 426–432, Oct. 2018, doi: 10.1021/acs.jpcc.8b08547.

4 Chapter 4 – Conclusions

4.1 Summary of main findings

This work explored the potential of lignin-derived electrospun carbon mats as sustainable electrode substrates for electrochemical applications, with a specific focus on glycerol electrooxidation in alkaline media.

Electrospinning of organosolv lignin followed by carbonization produced free-standing carbon fiber networks characterized by a highly porous nonwoven architecture. Nitrogen adsorption measurements yielded a specific surface area of approximately 282 $m^2 g^{-1}$, while CO_2 adsorption revealed additional ultramicroporosity, resulting in an estimated surface area of around 517 $m^2 g^{-1}$. Pore size distribution analysis indicated that most of the porosity lies within the microporous region, while the fibrous architecture provides larger inter-fiber voids that facilitate electrolyte penetration and transport.

The influence of carbonization temperature on fiber morphology and carbon structure was investigated through SEM and Raman spectroscopy. Increasing the carbonization temperature resulted in progressive structural ordering of the carbon matrix, reflected by a decrease in the Raman I_D/I_G ratio. However, carbonization at 1200 °C produced brittle structures, whereas lower temperatures preserved mechanical integrity but showed a weaker electrochemical response, likely due to the higher amount of oxygen-containing functionalities retained in the carbon structure. Based on these observations, 1000 °C was selected as a compromise between structural ordering and mechanical stability.

Electrochemical characterization demonstrated that the lignin-derived mats can operate as stable electrode substrates in alkaline electrolyte. Compared with the commercial carbon paper benchmark (Freudenberg H23), the lignin-derived mats exhibited a higher capacitive background and enhanced electrochemical response, likely due to their higher accessible surface area and porous fibrous morphology.

When tested for glycerol electrooxidation in 1 M NaOH + 1 M glycerol, the lignin-derived mats showed higher oxidative currents than the commercial carbon paper, suggesting improved accessibility of catalytic sites and enhanced electrolyte transport within the fibrous network.

To address the intrinsic brittleness of the carbonized mats, carbon nanotubes were incorporated into the electrospinning formulation as a conductive reinforcement. Two CNT loadings were investigated (0.5 wt% and 0.75 wt% relative to solids in the precursor solution), corresponding to final CNT contents of approximately 1.4% and 2.2% after carbonization. Moderate CNT incorporation improved the electrochemical response, likely by enhancing electronic conductivity within the fibrous network. However, higher CNT loading led to aggregation phenomena observed in TEM images, which negatively affected the electrochemical performance.

Finally, SEM analysis performed before and after electrochemical testing revealed the formation of surface deposits along the carbon fibers after glycerol electrooxidation, likely associated with the accumulation of reaction intermediates or oxidation products. Despite these surface changes, the overall fibrous architecture of the lignin-derived mats remained largely preserved, indicating that the substrate maintains its structural integrity under the investigated electrochemical conditions.

Overall, this work demonstrates that lignin-derived electrospun carbon mats can function as effective free-standing electrode substrates and highlights their potential, beyond the specific case of glycerol electrooxidation, as renewable alternatives to fossil-derived carbon substrates in electrochemical devices.

4.2 Limitations of the present work

Despite the promising results obtained in this study, several limitations of the present work should be acknowledged.

First, the electrochemical investigation was mainly limited to cyclic voltammetry measurements. While these experiments provide useful insights into the electrochemical behavior of the materials, a more comprehensive evaluation of electrode durability under

prolonged operation was not performed. Long-term stability tests would therefore be necessary to assess the robustness of the developed electrodes under realistic operating conditions.
Second, the electrospun carbon mats exhibit a relatively low packing density due to their highly porous fibrous structure. Although this architecture is advantageous for electrolyte accessibility and mass transport, it may limit volumetric performance and mechanical robustness when compared to more compact electrode supports.
Another limitation concerns the absence of a quantitative mechanical characterization of the carbon mats. While qualitative observations indicate that the materials can become brittle depending on the carbonization conditions, systematic measurements of mechanical properties such as tensile strength or flexibility were not performed in this work.
Finally, the present study focused primarily on electrochemical activity, while the products generated during glycerol electrooxidation were not quantitatively analyzed. In addition, although SEM observations suggest the formation of surface deposits after electrochemical operation, the precise chemical nature of these species remains unresolved and would require further surface characterization techniques.

4.3 Future perspectives for lignin-based electrospun carbon substrates as alternatives to fossil-derived supports

The results obtained in this work highlight several promising directions for the further development of lignin-derived electrospun carbon mats as sustainable electrode substrates for electrochemical applications.
One important aspect concerns the structural optimization of the fibrous carbon network. The electrospun mats developed in this study exhibit a highly porous architecture that promotes electrolyte accessibility and mass transport. However, the same structure results in relatively low packing density, which may limit volumetric performance and mechanical robustness in practical electrochemical devices. Increasing the density of electrospun carbon mats while preserving their hierarchical porosity could therefore represent an important design parameter for future electrode architectures.
Strategies to increase the density of lignin-derived electrospun carbon materials have already been reported in the literature. In particular, Hérrou et al. demonstrated that stacking and compressing electrospun lignin nanofiber mats prior to carbonization can significantly increase the material density and improve volumetric performance in electrochemical systems (Figure 28).

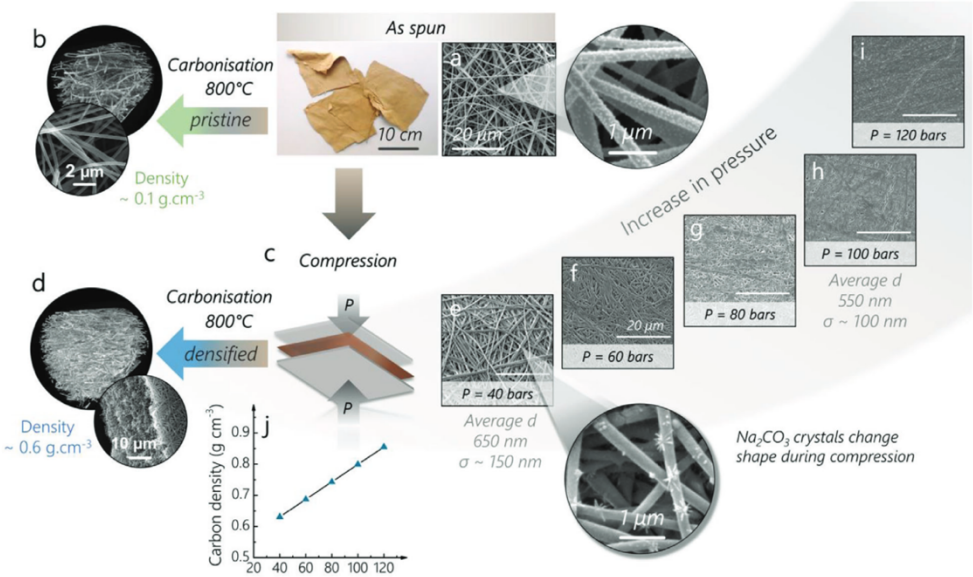

Figure 28 - Strategy for increasing the density of lignin-derived electrospun carbon mats through stacking and compression prior to carbonization, enabling higher volumetric performance. Reproduced from Hérrou et al., Advanced Science (2023).

Such an approach could represent a promising strategy to enhance the mechanical stability and structural integrity of lignin-derived carbon electrodes.

From an electrochemical perspective, further studies should also investigate the influence of catalyst loading and electrode architecture on the overall reaction performance. In particular, increasing the platinum loading or optimizing catalyst deposition strategies could provide additional insights into the catalytic capabilities of lignin-derived carbon substrates.

Another key aspect for future research is the evaluation of long-term electrode durability. While cyclic voltammetry measurements demonstrated stable electrochemical behavior in alkaline electrolyte, extended durability tests under continuous operation would be required to assess the long-term stability of the electrodes under realistic electrochemical conditions.

In addition, the present study primarily focused on electrochemical activity, while the reaction products generated during glycerol electrooxidation were not quantitatively analyzed. Future investigations should therefore include product identification and selectivity analysis, for example through chromatographic techniques, in order to better understand the reaction pathways occurring on these electrode systems.

Finally, advanced surface characterization techniques could be employed to investigate the evolution of the electrode surface during catalysis. Although SEM observations suggest the formation of surface deposits after electrochemical operation, the precise chemical nature of these species remains unresolved. Techniques such as XPS or elemental mapping could provide valuable insight into catalyst–support interactions and the evolution of surface chemistry during electrochemical glycerol oxidation.

Overall, continued optimization of material structure, catalyst integration and electrochemical characterization could further establish lignin-derived electrospun carbon mats as promising sustainable alternatives to conventional fossil-derived carbon electrode supports.

Acknowledgements

I would like to express my sincere gratitude to **Prof. Magda Titirici** for giving me the opportunity to carry out this research within her group at **Imperial College London** and for fostering such an inspiring scientific environment.

The Titirici Group provided a welcoming atmosphere, a continuous exchange of ideas and a stimulating research environment that made this experience particularly enriching.

Special thanks go to **Dr. Robert Hunter** and **PhD candidate Hanzhi Ye** for their close supervision during this project. Their guidance, insightful discussions and constant encouragement during the experimental work were invaluable to the development of this thesis.

I would also like to sincerely thank **Prof. Marco Sangermano** for his teaching during my studies and for making it possible for me to undertake this work at Imperial College London under his supervision. His thoughtful guidance and steady presence throughout this journey have been deeply appreciated.

I would also like to acknowledge all the wonderful people I met during my studies. In particular, I am deeply grateful to **Sofia, Valentina, Mattia, Stefano, Pierpaolo, Marianna, Giovanni, Pietro and Alessandro** for their friendship, encouragement and for the many moments we shared along the way. A special thank you also goes to **Bailey J. Mills**.

My deepest gratitude goes to my family **Luljeta, Astrit, Giulia, Engy, Tiziano, Giulio, and the soon-to-arrive Niccolò** for their unconditional support and for always giving me the strength to move forward.

Finally, I would like to thank my partner, **Louis**, for his love, patience and unwavering encouragement throughout this journey.